AN INVESTIGATION OF THE PROPERTIES AND INFLUENCE OF WAVE-INDUCED ORGANIZED MOTION IN THE ADJACENT AIRFLOW

ALLEN JESTEN FRANK

LIBRARY
NAVAL POSTGRADUATE SCHOOL
MONTEREY, CALIF. 93940

United States
Naval Postgraduate School

LIBRARY
NAVAL POSTGRADUATE SCHOOL
MONTEREY, CALIF. 93940

THESIS

AN INVESTIGATION OF THE PROPERTIES AND INFLUENCE
OF
WAVE-INDUCED ORGANIZED MOTION IN THE ADJACENT AIRFLOW

by

Allen Jesten Frank

Thesis Advisor: K. L. Davidson

September 1971

Approved for public release; distribution unlimited.

An Investigation of the Properties and Influence of Wave-Induced Organized Motion in the Adjacent Airflow

by

Allen Jesten Frank
Lieutenant Commander, United States Navy
B.S., University of Kansas, 1961

Submitted in partial fulfillment of the
requirements for the degree of

MASTER OF SCIENCE IN METEOROLOGY

from the

NAVAL POSTGRADUATE SCHOOL
September 1971

ABSTRACT

Turbulence data obtained over natural water waves were analyzed using joint probability distribution and conditional means methods. These data represented conditions when the waves were decaying and when the waves were building. In both cases, significant wave-induced fluctuations were identified in the airflow. All features of the velocity fluctuations were examined for two levels above mean water level. In the case of a decaying wave field, decelerations in the airflow can be associated with an assumed propagating pressure maximum over the crest of the wave. Other than this deceleration, the airflow appears to reflect simple streamline bending over the mobile irregular wave surface. In the case of a building wave field, velocity fluctuations appear to agree with those predicted by linear wave generating theories.

TABLE OF CONTENTS

I. INTRODUCTION 8

II. THEORETICAL CONSIDERATIONS 11

A. WIND-WAVE COUPLING 11

B. STATISTICAL CONSIDERATIONS AND PROCEDURES 14

1. Normalization and Computation of Statistics 17

2. Bandpass Filter 17

3. Computation of JDF/CMF 18

4. Checks for Filter and Random Noises 20

5. Theory and Computation of Phase Amplitude 22

III. DESCRIPTION OF DATA 27

A. LOCATION AND DESCRIPTION OF THE TOWER 27

B. INSTRUMENTATION AND SENSOR MOUNTING ARRANGEMENT 30

IV. PRESENTATION AND INTERPRETATION OF RESULTS 34

A. RESULTS FOR 19 AUGUST 36

B. RESULTS FOR 26 SEPTEMBER 51

V. CONCLUSIONS AND RECOMMENDATIONS 65

APPENDIX A: JDF/CMF COMPUTER PROGRAM 67

APPENDIX B: TEMPERATURE JDF/CMF ANALYSES 69

BIBLIOGRAPHY 79

INITIAL DISTRIBUTION LIST 81

FORM DD 1473 83

LIST OF FIGURES

1. Summaries of Drag Coefficients Versus Wind Speed 10

2. Streamlines of Sinusoidal Perturbation in a Shear Flow Near $Z = Z_c$; (a) Kinematic Consequence, (b) Consequence of Dynamics of Critical Level, Which is a Streamline Shift ... 13

3. JDF/CMF Smoothed Output Array 16

4. Response Curve for Inverse Transform Filter, 59 Pt. 18

5. Analyzed JDF/CMF for Random Numbers 20

6. Analyzed JDF/CMF for; (a) Bandpassed Data, (b) Non-bandpassed Data 21

7. JDF/CMF Smoothed Output Array Depicting the Octants for Phase-Amplitude Computations and 1.5σ Boundaries (Box Around Center) for Separating Large and Small Amplitude Waves 25

8. Location of U.S. Lake Survey Research Tower; (a) Lake Michigan, (b) Tower Site near Muskegon, Michigan 28

9. Research Tower; (a)as Instrumented During Experiment, (b) Schematic Showing Underwater Tripod Support Structure 29

10. Sensor Mounting Arrangement on Tower; (a) Components and Vertical Array, "Plumbline", (b) Picture of Sensors During Measurement Period 32

11. Picture of Capacitance Wave Gauge and Bridge-Amplifier System 33

12. General Conditions for 19 August 1968 37

13. General Conditions for 1226 to 1244 CST, 19 August 1968 38

14. Velocity Variance and Covariance Results and Wave Spectra (with Bandpass Filter Superimposed) for 19 August 1968, with 1.5 Meter Level on the Left and 4.0 Meter Level on the Right 39

15. Streamlines for Potential Flow; (a) Simple Bending of Streamlines, (b) Relations Between u and w in Potential Flow 41

16. U-W JDF/CMF Results for 1.5 Meters for 19 August 1968 43

17. U-W JDF/CMF Results for 4.0 Meters for 19 August 1968 44

18. Phase-Amplitude Results for 1.5 Meters; (a) Small Waves, (b) Large Waves, (c) All Waves for 19 August 1968 47

19. Phase-Amplitude Results for 4.0 Meters; (a) Small Waves, (b) Large Waves, (c) All Waves for 19 August 1968 48

20. Phase-Amplitude Results for Sine Waves Utilizing Spectral Analysis Phase Angles; (a) 1.5 Meters, (b) 4.0 Meters for 19 August 1968 50

21. Summary Illustrating Probable Cause for the Distortion in the u Component for 19 August 1968 52

22. General Conditions for 26 September 1968 54

23. General Conditions for 1355 to 1413 CST, 26 September 1968 55

24. Velocity Variance and Covariance Results and Wave Spectra (with Bandpass Filter Superimposed) for 26 September 1968, with 1.5 Meter Level on the Left and 4.0 Meter Level on the Right 56

25. U-W JDF/CMF Results for 1.5 Meters for 26 September 1968 57

26. U-W JDF/CMF Results for 4.0 Meters for 26 September 1968 58

27. Phase-Amplitude Results for 1.5 Meters; (a) Small Waves, (b) Large Waves, (c) All Waves for 26 September 1968 60

28. Phase-Amplitude Results for 4.0 Meters; (a) Small Waves, (b) Large Waves, (c) All Waves for 26 September 1968 61

29. Phase-Amplitude Results for Sine Waves Utilizing Spectral Analysis Phase Angles; (a) 1.5 Meters, (b) 4.0 Meters for 26 September 1968 63

30. JDF/CMF Results; $W_{1.5}$ and $T_{1.5}$ with Waves for 19 August 1968 .. 69

31. JDF/CMF Results; $W_{4.0}$ and $T_{4.0}$ with Waves for 19 August 1968 .. 70

32. JDF/CMF Results; $U_{1.5}$ and $U_{4.0}$ with Waves for 19 August 1968 .. 71

33. JDF/CMF Results; $W_{1.5}$ and $W_{4.0}$ with Waves for 19 August 1968 .. 72

34. JDF/CMF Results; $T_{1.5}$ and $T_{4.0}$ with Waves for 19 August 1968 .. 73

35. JDF/CMF Results; $W_{1.5}$ and $T_{1.5}$ with Waves for 26 September 1968 74

36. JDF/CMF Results; $W_{4.0}$ and $T_{4.0}$ with Waves for 26 September 1968 75

37. JDF/CMF Results; $U_{1.5}$ and $U_{4.0}$ with Waves for 26 September 1968 76

38. JDF/CMF Results; $W_{1.5}$ and $W_{4.0}$ with Waves for 26 September 1968 77

39. JDF/CMF Results; $T_{1.5}$ and $T_{4.0}$ with Waves for 26 September 1968 78

ACKNOWLEDGEMENTS

The author wishes to take this opportunity to express his appreciation to his advisor, Professor K. L. Davidson, for his support, advice, and guidance throughout this research.

Appreciation is also expressed to Professor N. E. Boston for his careful review of the manuscript and useful suggestions, and to Dr. Jack Kaitala for his guidance in computer programming.

To the Printing and Graphics divisions of the Educational Media Department for their kind assistance, and to the W. R. Church Computer Facility of the Naval Postgraduate School for the free use of the IBM 360 Computer, my heartfelt thanks.

Finally, to my wife Melba, for her understanding and love, and my sons James, William, and Roger a very grateful, thank you.

I. INTRODUCTION

This study examines turbulence data obtained over natural water waves in order to determine the influence of the waves on the overlying air. The data examined are simultaneous measurements of velocity and temperature fluctuations at two fixed levels above mean water level.

The study extends a previous analysis on data for which significant evidence of wave-induced motion in the airflow was obtained. Joint probability density and conditional mean analysis are the statistical procedures used to extend the previous interpretations.

The lack of good descriptions of the interaction between the ocean surface and the adjacent air layer is a major obstacle preventing solution of a wide class of applied geophysical problems such as weather prediction and general circulation studies. A suitable description requires the application, to observational data, of specific statistical methods which could reveal properties of wave-induced organized motion.

Current problems requiring additional knowledge on the dynamics of the surface layer are the determination of:

1. kinetic energy dissipated by boundary layer turbulence;

2. thermal energy gained by turbulent transport of sensible and latent heat;

3. energy transformed by vertical velocities due to the horizontal distribution (convergence) of surface friction; and

4. surface winds used in semi-empirical wave forecasting models.

Although numerous observational investigations have been conducted to describe the structure of the near surface layer, the majority of these measurements have been over land. Therefore, parameterization of the

boundary layer over the sea has been based on overland results. It is clear, however, that a mobile irregular wave surface receiving kinetic energy from the airflow can influence the turbulent regime within the adjacent airflow. Therefore, empirical formulae, valid or at least tested over land, may not be valid over water.

Examples of the conflicting results obtained from strictly empirical approaches appear in Figure 1 in which various proposed drag coefficient relations are presented for over the water. Being able to add some dynamical description to this region should help in narrowing ones' choices for this empirical coefficient.

Data used in this study were previously analyzed by Davidson (1970). However, those analyses consisted of spectral analyses and the limitations imposed on the interpretation of spectral results hindered the description of several important properties of the observed organized motion. Procedures employed in the present study are well suited for examining organized motion within a turbulent regime. The statistical procedures (Holland, 1968) were designed to reveal systematic structure in various types of meteorological data but at the present time have only been applied to larger scale fluctuations. This study is the first attempt to apply these procedures to small scale fluctuations.

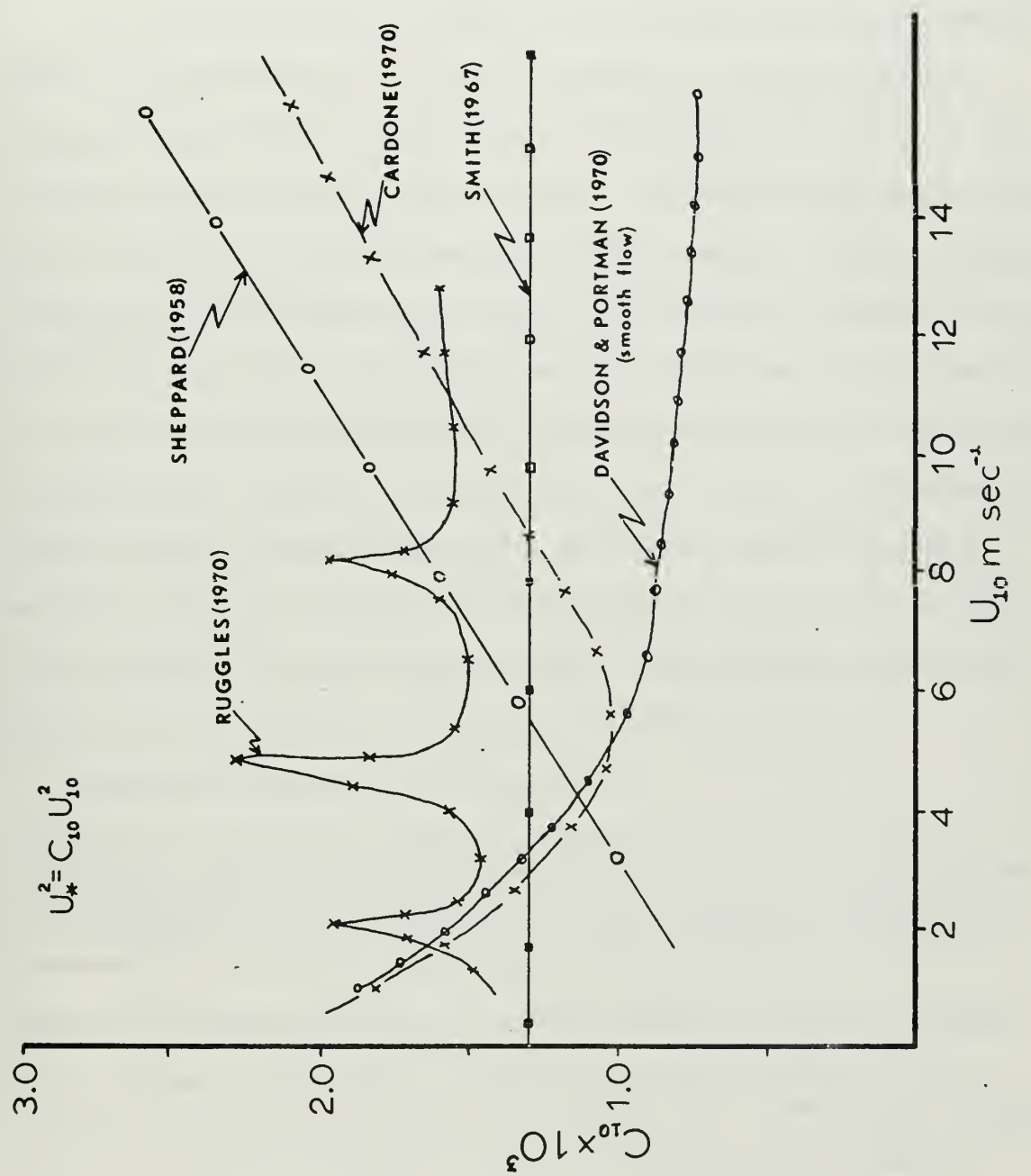

FIGURE 1. Summaries of Drag Coefficients Versus Wind Speed

II. THEORETICAL CONSIDERATIONS

A. WIND WAVE-COUPLING

In a survey of the understanding of the airflow over water, Stewart (1967) forewarned that the air-water boundary is not "just another boundary layer", but is unique in that the interface is a part of the solution for the boundary layer airflow. The interface is free to move and, as observed, it takes advantage of this freedom. Stewart, evaluating existing wave generation models (Miles and Phillips), indicated that in 1967 there were still insufficient overwater measurements to either verify or invalidate existing analytical theories of the interaction between a turbulent shear flow and the underlying water surface. He reported, however, that even though he examined a very large number of overwater velocity spectra, in no case were there sharply defined spectral peaks corresponding to the wave spectra peaks. Other studies, however, have revealed the existence of wave-induced motion in the air.

Yefimov and Pososhkov (1969) reported:

> "Laboratory experiments indicate that surface waves induce in initially quiet air not only periodic velocity fluctuations but also stationary flow in the direction of wave propagation. The velocity of stationary flow is considerably higher than would follow if we assumed it to resemble Stokes wave flow in the water."

Volkov (1969) reported, based on interpretations of spectral results:

> "... the wave surface has a considerable influence on all of the statistical characteristics of turbulence in the atmospheric boundary layer - the fluctuation spectra and dispersion, the turbulent fluxes, etc. We therefore succeed in finding some typical features and regularities of this influence by the complex method of investigating the processes of interaction between the atmospheric boundary layer and the agitated sea surface."

Davidson (1970), also interpreting spectral results, concluded:

> "... analyses of the boundary layer over a majority of the earth's surface cannot be based on the assumption that the surface is a rigid boundary. The influence of the waves on the adjacent airflow has been found to be too significant to rely on over-land data to describe the boundary layer over waves. Reliable empirical relations giving the flux of momentum as a function of the wind profile and density gradients will have to be formulated from data obtained over the ocean surface itself."

An analytical model describing coupling between a wave surface and the overlying air flow was first proposed by Miles (1957). In this model, the wave-induced perturbation is considered in a coordinate system which is stationary with respect to the wave (i.e., surf-rider's coordinate system moving at the phase speed c). Streamlines in such a coordinate system would appear as in Figure 2. The Miles' critical height (dashed line) occurs at the level where the wind speed is equal to the wave speed. The wave, Figure 2, is stationary in this coordinate system; therefore, below the critical level the air appears to move to the left since it moves slower than the waves. Above the critical level, where the wind speed is greater than the phase speed, the air moves to the right.

The Miles mechanism can be described as a positive feedback mechanism and, as such, it depends on the pre-existence of the wave. Forces within the Miles theory leading to wave growth are depicted in Figure 2. Region A is a region of negative vortex acceleration and Region B is one of positive vortex acceleration, but the absolute value of the vortex acceleration is greater at point A than at B. Therefore, there is a negative vortex acceleration at that level hence a deceleration of the mean wind when averaged over a wave length. This deceleration results in a loss of momentum from the airflow which contributes to the momentum increase of the wave.

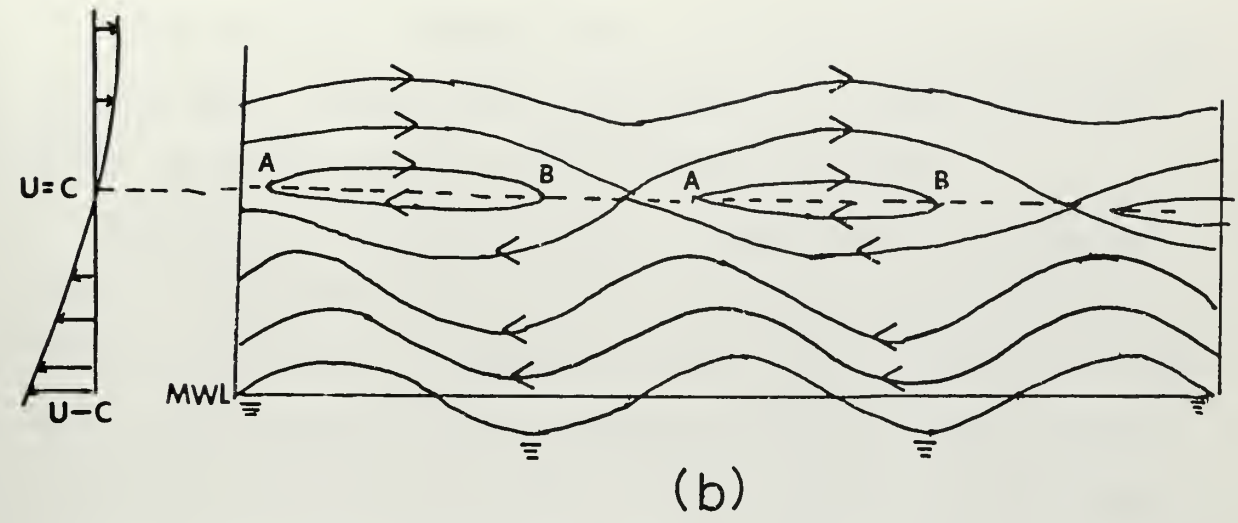

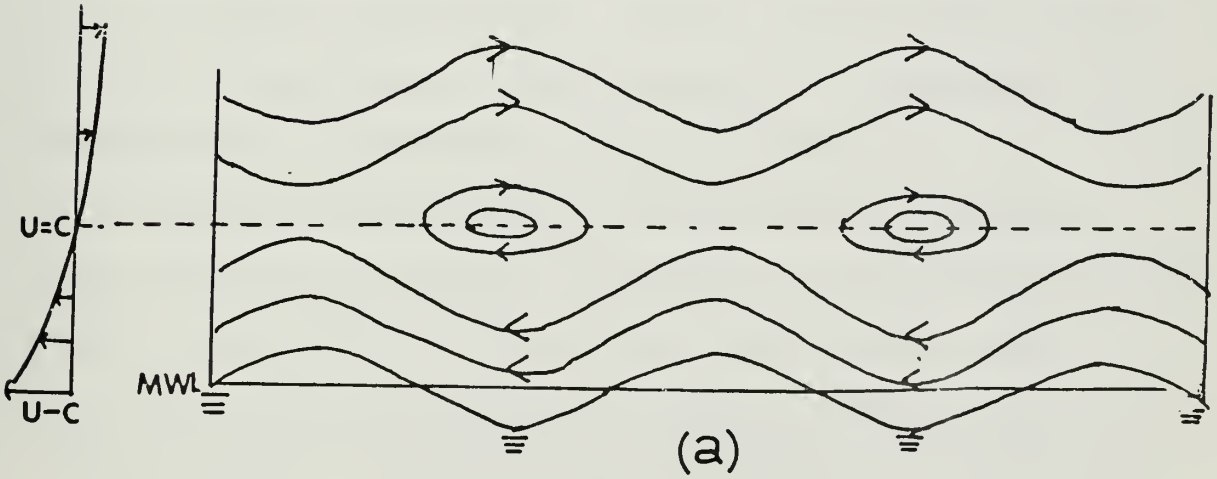

FIGURE 2. Streamlines of sinusoidal perturbation in a shear flow near $Z = Z_c$; (a) kinematic consequence, (b) consequence of dynamics of critical level.

It has been shown (Kinsman, 1965, p. 571) that the kinematics at the critical level, described above, would result in a phase shift, with height, of the wave-induced vertical velocity component.

Therefore, it is observed, within a linear model, that the wave-induced fluctuations can be important in altering momentum transfer in the air layer adjacent to the waves. Also, specific predictions of this theory can be examined, such as a phase shift of the vertical velocity with respect to height. It should be noted, however, that within this investigation possible non-linear interactions between the wave-induced motion and the shear flow will also be examined.

B. STATISTICAL CONSIDERATIONS AND PROCEDURES

Statistical procedures used in this study were described by Holland (1968). Applied to three variables, these procedures yield the joint probability density function (JDF) for a pair of the variables with a conditional mean function (CMF) of a third variable.

Holland argued convincingly on the suitability of this type of analysis for turbulent regimes. In reference to the application of these procedures to a turbulent regime, Holland cited Batchelor (1953):

> "It is a premise of probability theory that a random function $f(\alpha)$, say, defined for all values of α, is determined statistically by the complete system of joint-probability distributions of values of the function at any n values of α, where n may take any integral value. Likewise, the infinite field of turbulent motion is determined statistically by the complete system of joint-probability distributions of the values of the vector velocity $\vec{u}(\vec{x},t)$ at any n points of of space-time."

A joint probability density function is a means to represent simultaneously observed values of pairs of variables by contours on a two-dimensional array. A trivariate statistical relationship is obtained by computing a conditional mean of a third variable as a function of the two

independent variables contributing to joint probability density function (JDF). This trivariate statistical relationship, hereafter denoted JDF/CMF, can therefore, be represented by two sets of contours on a two-dimensional array.

Joint probability density function and conditional mean function analysis results are illustrated in Figure 3. The array is centered on the mean value, which is zero, of the two variables. Each cell in the row or column consists of two numbers. The bottom number represents the JDF, the probability ($x10^3$) of the joint occurrence of the representative deviation for the pair of variables, and the upper number represents the CMF, the mean of the third variable corresponding to the given joint occurrence of the pair.

These results have been smoothed by a nine-point smoother to remove the perturbations viewed as being physically and statistically insignificant. This smoothing reduced an 18 by 18 array to the observed 16 by 16 array.

The following list of steps within the JDF/CMF statistical procedures will be described in the ensuing paragraphs:

1. normalization and computation of preliminary statistics of the variables;
2. bandpass filtering;
3. computation of JDF/CMF;
4. checks for filter and random noise; and
5. computation of phase-amplitude information.

Computation and plotting of all statistics were done in the W. R. Church Computer Facility[1] of the Naval Postgraguate School.

---

[1]The analysis utilized the IBM 360 Computer and a CALCOMP plotting device for the computations and contour plotting.

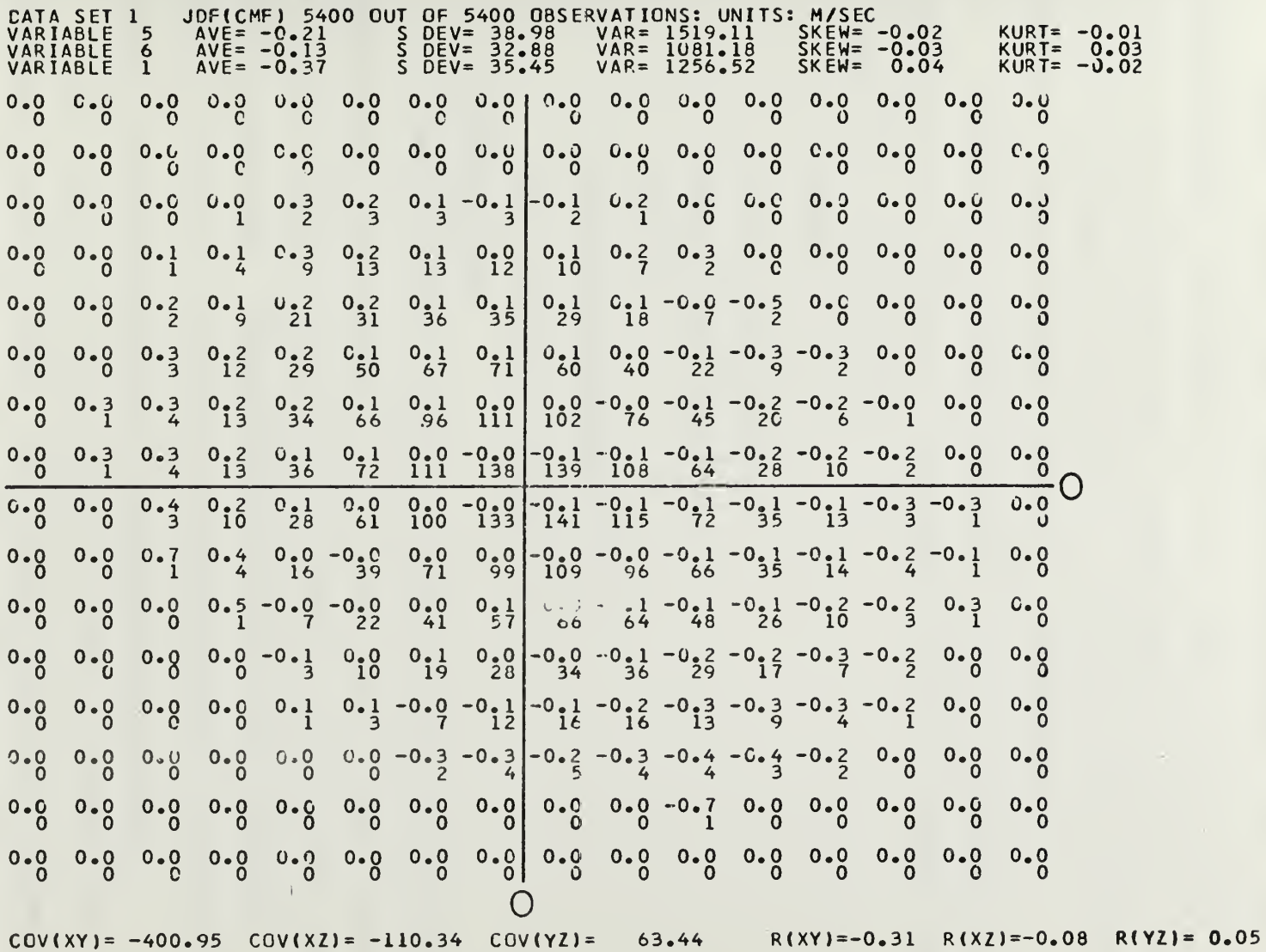

FIGURE 3. JDF/CMF Smoothed Output Array

1. Normalization and Computation of Statistics

JDF/CMF statistics were computed from normalized values of the original variables. For example, if x (i) = values in one of the three sets, $\bar{x}$ = mean of all x(i), and σ = standard deviation of all x(i), the JDF and CMF were computed for $(x(i)-\bar{x})/\sigma$. Normalized values were obtained for each of the three variables included in a JDF/CMF analysis.

In addition to the mean and standard deviation, other statistics were computed and tabulated for each variable and pairs of variables used in the analysis. These statistics were:

1. variance;
2. skewness of each variable;
3. kurtosis of each variable;
4. covariances;
5. correlation coefficients; and
6. number of data points used.

2. Bandpass Filter

A bandpass filter was applied in order to isolate the significant frequency band (0.1Hz to 0.8Hz) as indicated by previous spectral analysis on the data (Davidson, 1970). There were several numerical filters that could have been used. Investigation revealed that the most desirable filter, with respect to sharpness of cutoff and magnitude of oscillations beyond the terminal frequency, was an inverse transform filter.

The response curve for the inverse transform bandpass filter with 59 weights is shown in Figure 4. The filter is superimposed (Figure 14) on the wave spectra, also shown are the velocity variance and covariance spectra. The filter passes a range of frequencies from about 0.1 Hz to 0.8 Hz.

The application of this bandpass filter enabled analyses of wave-induced fluctuations without contamination by higher and lower frequency fluctuations.

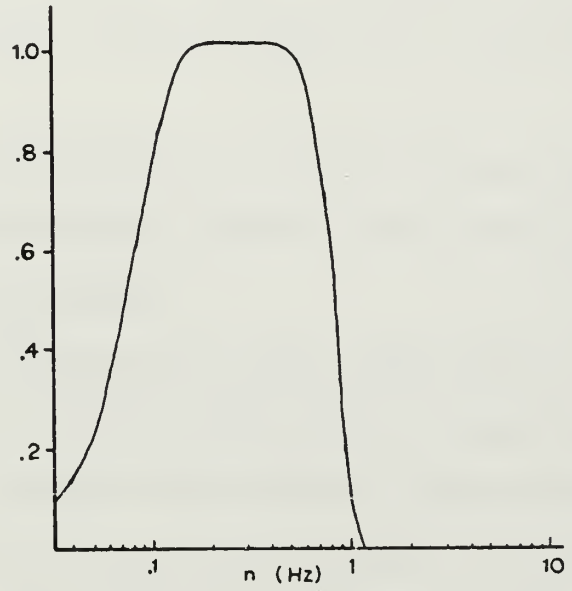

FIGURE 4. Response Curve for Inverse Transform Filter, 59 Pt.

3. Computation of JDF/CMF

A JDF represents the probability of a joint occurrence for a pair of variables. Therefore, for each pair of variables two indices were computed representing the position of simultaneously observed values of the variables in an 18 by 18 array of $\sigma/2$ by $\sigma/2$ joint class interval. For example, if the first values in the two sets were 1.25 and 0.9 standard deviations from their respective means, their joint occurrence would be tabulated in the $\sigma/2$ by $\sigma/2$ cell with indices (3,2). The CMF was computed for each joint class interval and was the average value of the third variable in the set for all observation times when the two independent variables had values within the joint interval.

An additional step in these procedures was to divide the number of joint occurrences by the total number of observations. This gave the probability per $\sigma^2/4$ within each cell of the 18 by 18 array which was then smoothed to a 16 by 16 array. Likewise, the sums of the third variable were divided by the number of joint occurrences in each cell. This yielded the average deviation from the mean of the third variable corresponding to a particular probability per σ^2 for the other two variables.

The output was printed out in a 16 by 16 array, Figure 3, and the array was analyzed by Contour, a computer library subroutine, and plotted on the CALCOMP plotting device.

An analyzed JDF/CMF (for a random number field) is illustrated in Figure 5. The contours connect equal values of occurrences in the JDF. They are concentric circles because they were generated from a random number field and circles indicate (as expected) no relationship between the two variables making up the JDF. A statistical relationship between two variables, other than between orthogonal relations such as a sine and cosine, would cause asymmetrical or elliptical contours. The heavier lines in this two-dimensional picture represent isolines of the CMF with the heaviest (dashed) being the zero line. An analysis with this degree of complexity, containing essential relations which exist among three variables, is not difficult to read with comprehension.

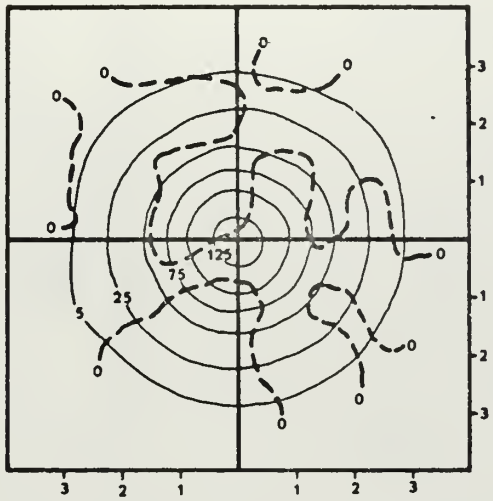

FIGURE 5. Analyzed JDF/CMF For Random Numbers

Any pair of variables can be used to compute the JDF and any variable can be used to compute the CMF. In Figure 25, the JDF is u and w denoted by (u,w) and the CMF is η as a function of u and w. The JDF/CMF is denoted by η (u,w).

4. Checks for Filter and Random Noises

Bandpass filtered data were analyzed and compared to the unfiltered data to insure that the data were not altered by the bandpass filter. The analysis of the same variables for the bandpassed (A) and the non-bandpassed (B) data are shown in Figure 6. It can be seen that the JDF (asymmetrical circles) for the two sets of data are essentially the same. CMF features in the bandpassed analysis are smoothed versions of those in the non-bandpassed analysis. The resultant differences between A and B are differences that could be caused by the addition of random numbers (which is essentially the contribution from background turbulence) onto the data.

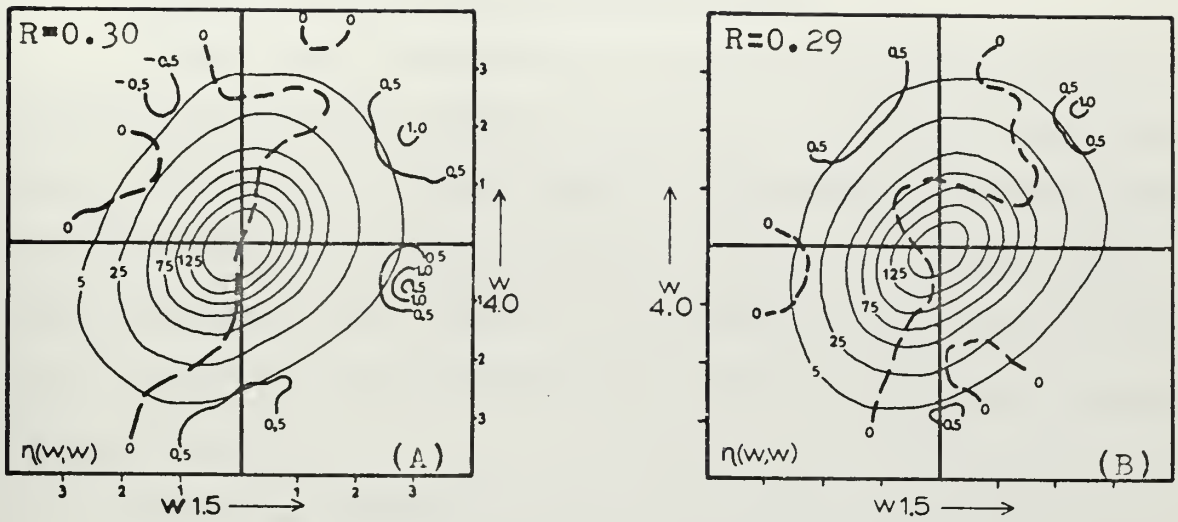

FIGURE 6. JDF/CMF of Filtered (A) Data and Unfiltered (B) Data

As a test on the results, random numbers were superimposed on the data used in each analysis. The values of these random numbers were of the same order of magnitude as the data field itself. It was expected that by superimposing random numbers, as in Figure 5, onto a data field, such as Figure 17A, where there is some statistical relationship, there would result a final JDF like Figure 17B where the asymmetry would be decreased. This was done for each variable analyzed and such a result was indeed realized.

The analysis of each set of variables was done twice, once with the bandpassed data and once with a random number field superimposed on the bandpassed data. This allowed a comparison between the data and the data plus random numbers to examine if the significant modes within the results represented something other than chance occurrences.

5. Theory and Computation of Phase Amplitude

In this study, information was also desired on the statistical dependence of the various turbulent variables on the phase of the waves. Within the context of a JDF/CMF analysis, this would be, for each variable plotted (Figure 18), its conditional mean function with respect to the phase angle of the wave. Similar to the JDF/CMF results a method of display is required to emphasize particular variations and eliminate unwanted background noise.

An approach suggested by Holland was used in which the polar coordinates representing the amplitudes and phase angles of a variable can be determined by computing the JDF for a variable and its time derivative. This method for computing phase relations should reveal (Holland, 1968) if the phase relation between two variables shifts as a function of the amplitude of the reference variable. In particular, it will reveal if the amplitude of the dependent variable varies non-linearly with the amplitude of the independent variable. Such a result is highly significant in this study.

Holland defined for any fluctuating meteorological variable y a "statistical eddy period", τ_o , defined as

$$\tau_o = 2\pi \frac{\sigma_y}{\sigma_{\dot{y}}}$$

If the period of oscillation is τ , the ratio of the standard deviations can be found. If the variable is written as

$$y = A \sin 2\pi \frac{t}{\tau}$$

then

$$\dot{y} = \frac{2\pi A}{\tau} \cos 2\pi \frac{t}{\tau}$$

The means are both zero and the standard deviations are

$$\sigma_y = \frac{A}{\sqrt{2}}$$

and

$$\sigma_{\dot{y}} = \frac{2\pi A}{\sqrt{2}\,\tau}$$

therefore, it can be seen that

$$\frac{\sigma_y}{\sigma_{\dot{y}}} = \frac{\tau}{2\pi}$$

The statistical eddy period for each variable, the standard deviation of each variable and the standard deviation of the time derivative of each variable are given in Table 1.

	19 AUGUST			26 SEPTEMBER		
VAR.	σ_y	$\sigma_{\dot{y}}$	τ_o	σ_y	$\sigma_{\dot{y}}$	τ_o
η	25.03	8.10	3.88	8.91	4.11	2.72
U_L	26.97	10.02	3.38	39.92	14.65	3.42
W_L	22.13	7.91	3.52	17.78	7.72	2.89
T_L	0.04	0.01	3.22	0.16	0.06	3.42
U_u	27.86	9.30	3.76	41.56	14.48	3.61
W_u	23.26	8.67	3.37	26.68	10.54	3.18
T_u	0.04	0.01	3.13	0.10	0.04	3.36
$-UW_L$	636.25	304.66	2.62	1720.55	906.79	2.38
$-UW_u$	871.74	363.76	3.01	1759.83	820.39	2.70
WT_L	0.85	0.42	2.56	3.23	1.65	2.47
WT_u	0.87	0.44	2.50	3.93	1.83	2.70

TABLE 1. Statistical Eddy Period of Each Variable and Standard Deviations of Each Variable and its Time Derivative for 19 August and 26 September 1968

Phase results consisted of the statistical dependence of various turbulent variables on the phase of the waves (η). Therefore, a JDF coordinate system was used with η as the ordinate and its derivative ($\dot{\eta}$) as the abscissa. In this coordinate system, with the passage of a wave, η increases upward and successive values in time are higher on the right and lower on the left of the η-axis.

If the surface wave were a pure sinusoid, successive values of JDF ($\eta,\dot{\eta}$) would follow a counterclockwise circular path around the JDF coordinate system, passing through the extremes of η when crossing the $\dot{\eta}$-axis and through extremes in $\dot{\eta}$ when crossing the η-axis. However, water waves are not pure sinusoids so these paths would not necessarily be circular. They would, however, be less complicated than passages of eddies in a random turbulent regime.

The phase angle was defined by the angle measured (by octants) counterclockwise, Figure 7, from the positive $\dot{\eta}$-axis in the ($\dot{\eta},\eta$) coordinate system.

Phase relations were examined after separating the results into wave amplitude classes. The classes were defined by σ regions on the JDF array. In this case two amplitudes were considered, these being small amplitudes (less than 1.5σ) and large amplitudes (greater than 1.5σ). The numbered octants are shown in Figure 7 in which the box around the center represents 1.5σ. Essentially this permitted an examination of phase relationship with respect to large and small waves. In contrast, spectral analysis yields phase information as a function of frequency only, the amplitude being the mean amplitude at that frequency.

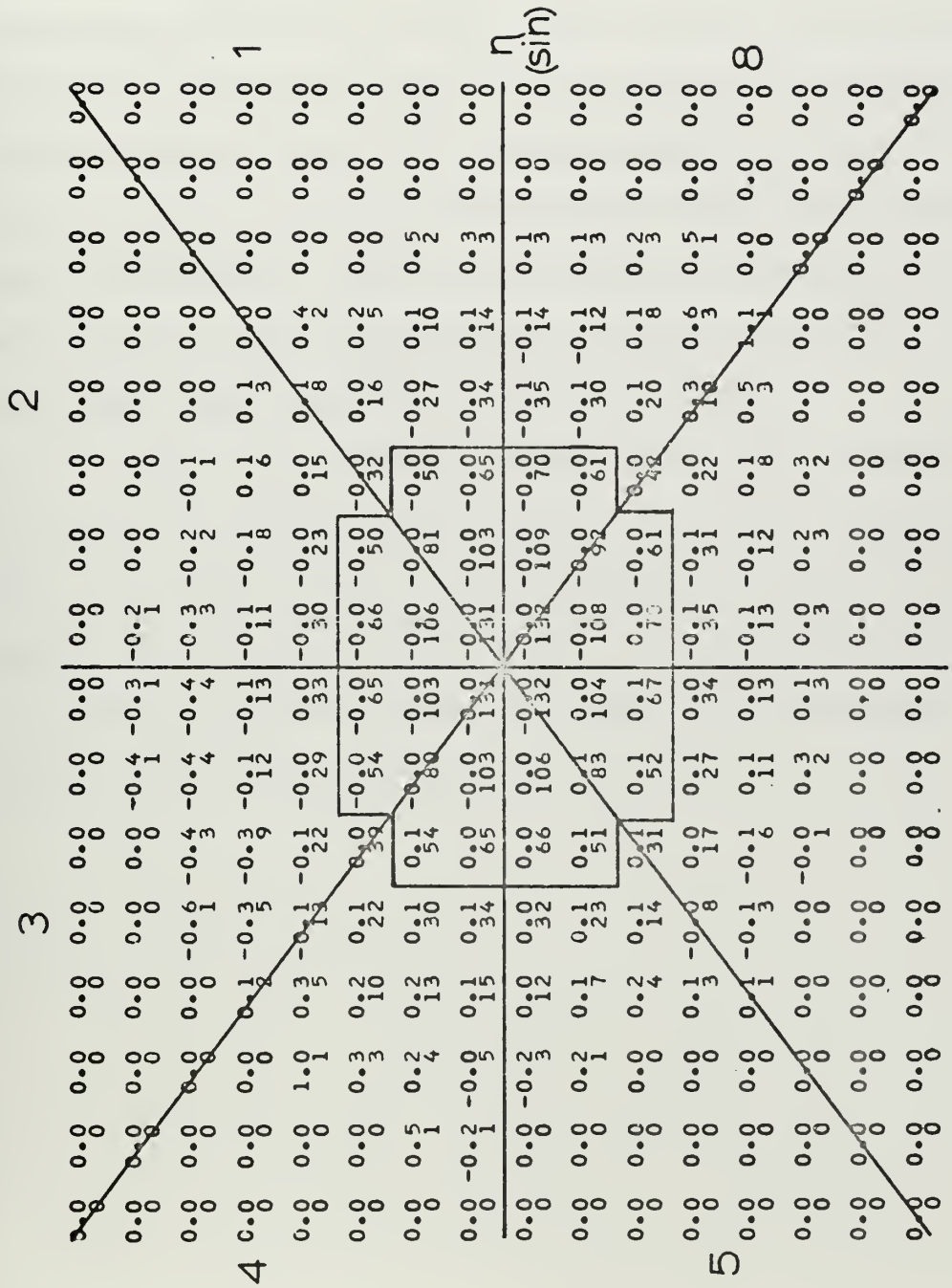

FIGURE 7. JDF/CMF Smoothed Output Array Depicting the Octants for Phase-amplitude Computations and 1.5σ Boundaries (Box Around Center) for Separating Large and Small Amplitude Waves.

Applying concepts of the above discussion, computations of the phase amplitude relations were made using the dependent variables as the conditional mean and the waves and time derivative of the waves as the independent variables for the JDF. After obtaining the JDF/CMF smooth array output, for example Figure 3, the products of the dependent variable (the upper number in each cell) and the probability function (the lower number in each cell) in all joint intervals of each octant and amplitude class were computed to obtain the amplitude stratified phase conditional mean function. This was done, Figure 18 bottom to top, for η, u, w, T, -uw, and wT, shown as horizontal bars for each octant.

A smooth curve was drawn through each set of horizontal bars so as to make the two areas between each bar and the curve approximately equal. These smooth curves were then analyzed for their phase relationship with the wave curve (bottom curve). The left hand set of curves (A) represents the small amplitudes. The middle set (B) represents the large amplitude and the right hand set (C) is the total of A and B.

III. DESCRIPTION OF DATA

The data examined in this study were from two days (19 August and 26 September 1968) of measurements on Lake Michigan by Davidson (1970). These were simultaneous measurements from a fixed tower, of wind (u and w) and temperature fluctuations and waves. The velocity and temperature measurements were obtained at two different levels above the mean water level. Waves were measured at a point directly below the air sensors.

A. LOCATION AND DESCRIPTION OF THE TOWER[2]

The measurements were made on Lake Michigan from a U.S. Lake Survey Research tower located in 15 meters of water 1.6 kilometers from shore near Muskegon, Michigan (Figure 8). Open water fetches at the tower location vary from 80 to 300 miles from the south clockwise through the northwest. Because the lake is not so large that separate weather systems and hence swell propagate from different directions, the local wave field was related to the wind field over the entire lake.

The general construction of the research tower and its instrumentation is shown in Figure 9. The structure, an open triangular truss, was designed both to achieve stability and to minimize disturbance to the air-flow and water motions. These were important considerations in the present analysis and interpretation. Stability was achieved by supporting the tower on the lake bottom by a tripod which was secured by a concrete anchor at each leg. The tower was also guyed in order to withstand extreme wind and wave conditions.

---

[2]An abridged version of the description by Davidson (1970).

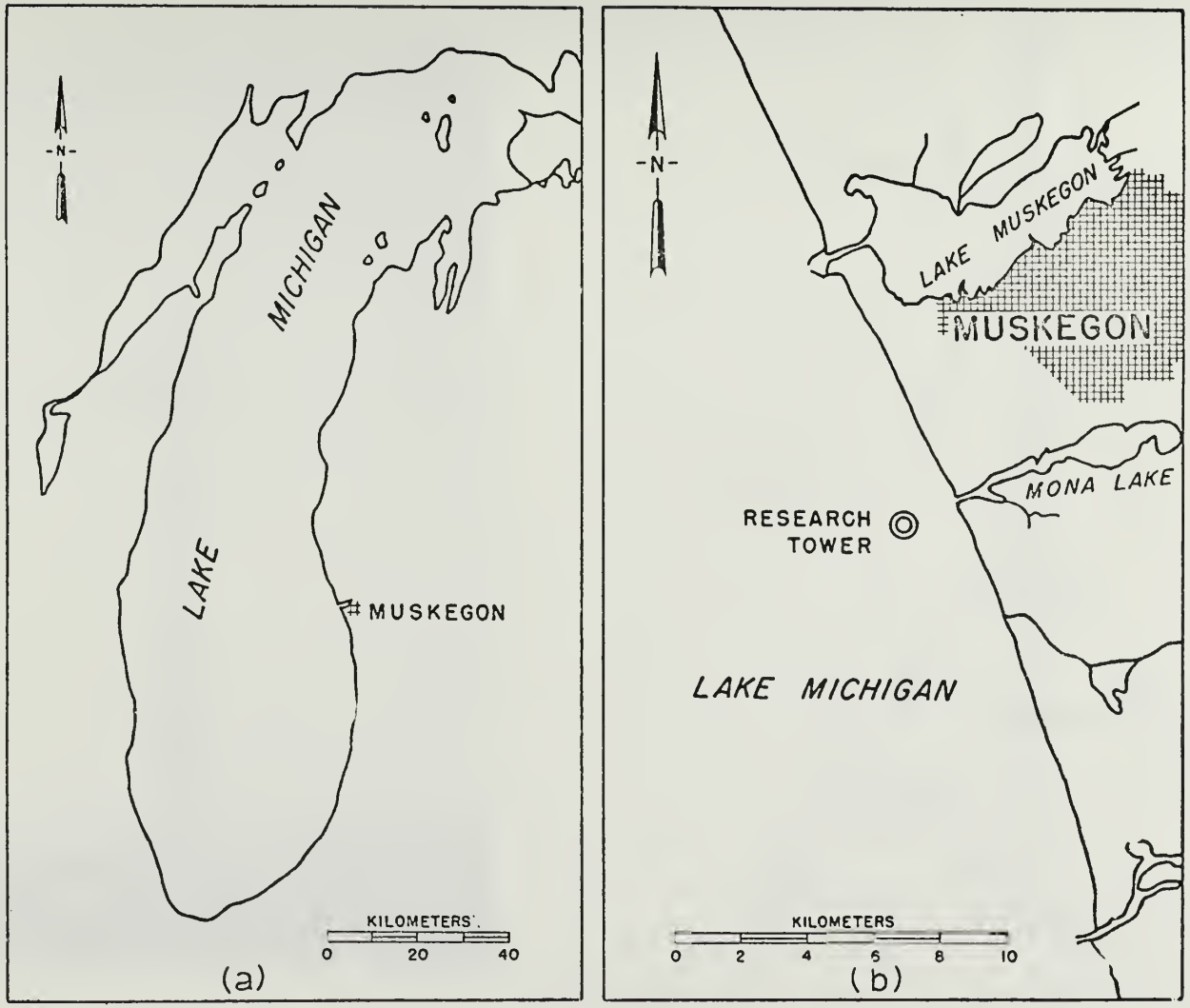

FIGURE 8. Location of U.S. Lake Survey Research Tower; (a) Lake Michigan, (b) tower site near Muskegon, Michigan.

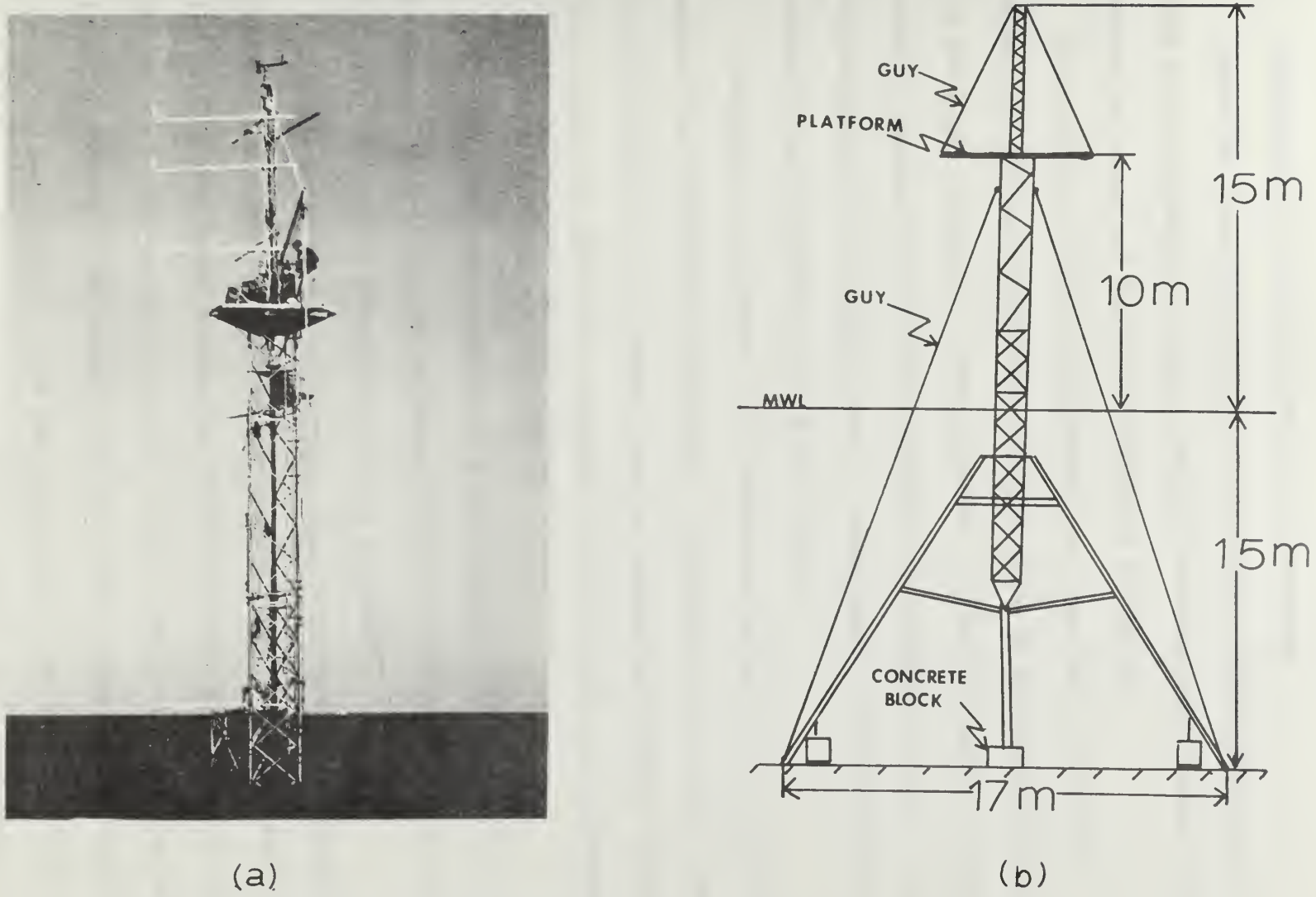

FIGURE 9. Research tower; (a) as instrumented during experiment, (b) schematic showing underwater tripod support structure.

B. INSTRUMENTATION AND SENSOR MOUNTING ARRANGEMENT

Figure 10A shows the features of the sensor mounting arrangement. A plumb line arrangement of sensors enabled determination of phase relations between the waves and turbulent components in the air.

The turbulent velocity measurements were made with a constant-temperature hot-wire anemometer using two wires in an X-configuration. The two wires arranged in X-configuration allowed the system to simultaneously measure the two wind components of interest (u and w). The probes were calibrated both in situ, based on simultaneous cup and propeller anemometer measurements, and in a wind tunnel.

A resistance thermometer, in a Wheatstone bridge circuit, was used to measure the temperature fluctuations. The output signal of the system was 125 millivolts for a one degree (Celcius) temperature change. Testing this system in a laboratory indicated it had the resolution to measure temperature to an accuracy of 0.05 C.

The waves were measured by a capacitance gauge and bridge system, Figure 11. The bridge was adjusted for full deflection, zero to one milliamp, between no immersion and full immersion.

The velocity and temperature sensors and wave gauge extended westward 2.5 times the width of the tower's side. Extension arms consisted of five centimeter rectangular tubing and were sturdy enough to avoid motion due to the airflow or waves. Also, a vertical pipe extended from below the water to two meters above the water so the sensors could be positioned at any height from the wave crest to two meters. Above the two meter level, arms were located at the four, eight, and fifteen meter levels.

Figure 10B is a photograph of the sensors mounted on the vertical pipe above the mean water level (MWL). A wind vane, such as that shown, was used at all levels to monitor the direction of the mean wind with respect to the sensors. The wave gauge can be seen directly below the hot wires in Figure 10B.

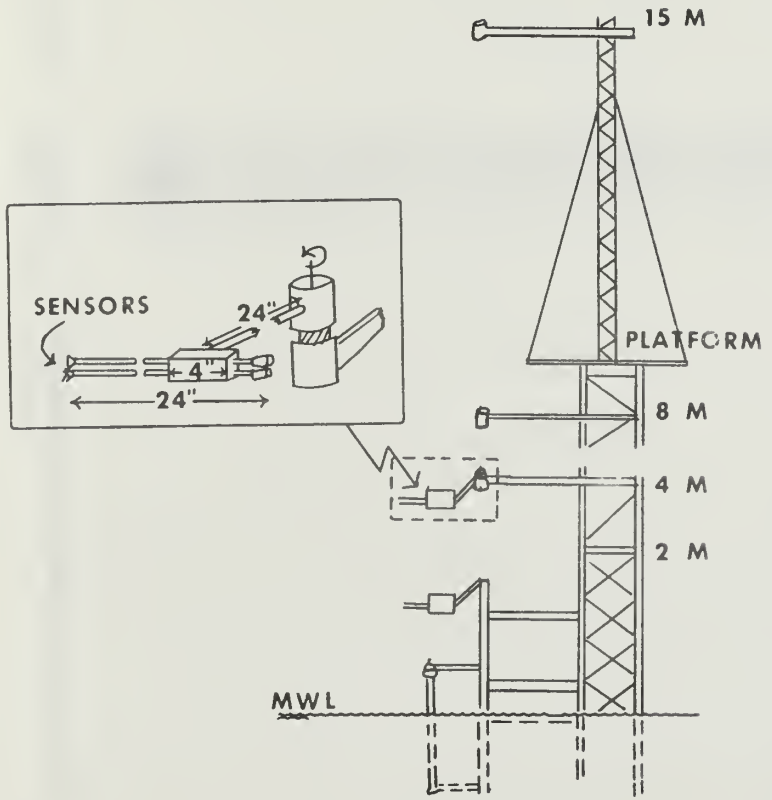

(a)

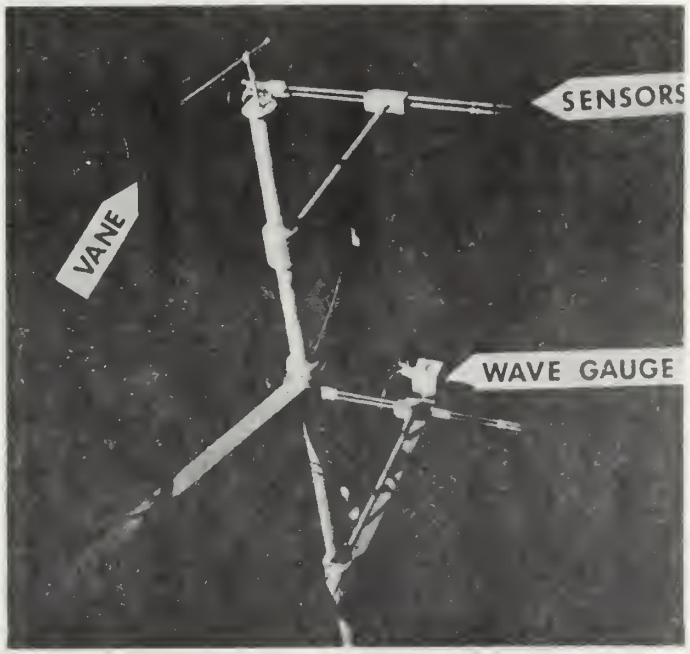

(b)

FIGURE 10. Sensor mounting arrangement on tower; (a) components and vertical array, "plumbline", (b) picture of sensors during measurement period.

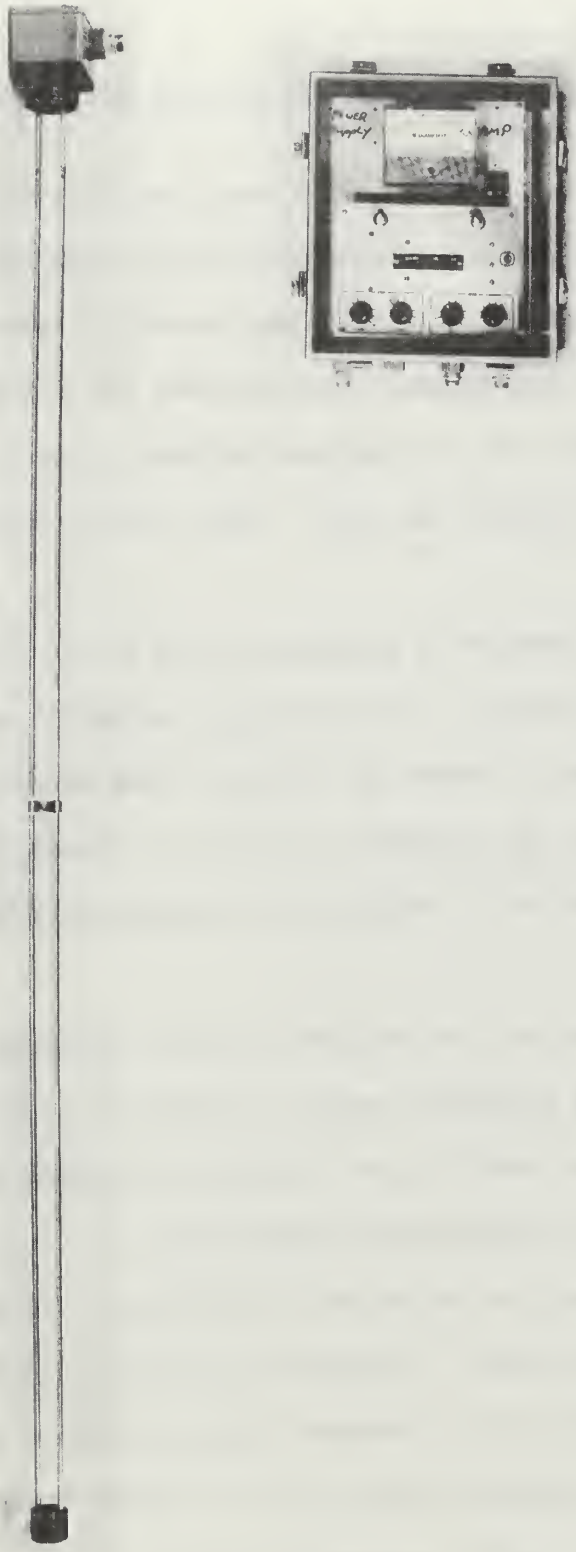

FIGURE 11. Picture of capacitance wave gauge and bridge-amplifier system.

IV. PRESENTATION AND INTERPRETATION OF RESULTS

In this section, JDF/CMF and phase amplitude results are presented and interpreted for the most probable relations between fluctuations in the airflow and the waves. Temperature relationships were also computed and a cursory examination has revealed some interesting fluctuations in the temperature field, but a detailed analysis of the temperature relationships was not performed in this study. They are included for reference in Appendix B.

Non-linear properties and phase relations of velocity fluctuations are emphasized in the following interpretation. Spectral results (Davidson, 1970) for these same data will be shown to complement the discussion. Spectral results are used to indicate the intensity of the observed wave-induced fluctuations with respect to the background, "normal" turbulent regime.

Interpretations obtained from the analyses of the present study should be viewed as significant extensions to those available from the previous spectral results. Although the spectral results show, according to frequency, the existence of wave induced fluctuations, interpretations are limited with respect to non-linear properties of the fluctuations and phase relations between fluctuating variables. Non-linear properties are not available within spectral results because of the inherent linear expansion, i.e., Fourier Series. Also, phase information, obtained from spectral analysis, is highly uncertain because of the high level of background, random turbulence at all the frequencies.

For each period, two figures are used to show JDF/CMF results and two figures are used to show phase amplitude results. Each of the two figures representing JDF/CMF results include a trivariate probability distribution from the following considerations of three variables, (η = waves, u = upper level, L = lower level),

1. $\eta(u_L, w_L)$
2. $\eta(u_u, w_u)$

within each of these figures, six plates (consisting of three pairs) are used to show the three possible combinations of the three variables. The pairs arise because all results are computed with and without the inclusion of random numbers. For example, six plates corresponding to the trivariate (1) above (where $\eta(u,w)$ means JDF of u and w with η as CMF) are:

Without Random Numbers	With Random Numbers
1. $\eta(u,w)$	4. $\eta(u,w)$
2. $w(\eta,u)$	5. $w(\eta,u)$
3. $u(\eta,w)$	6. $u(\eta,w)$

Phase-amplitude results are presented in two figures, one figure for all variables at each level and the wave. Each of these figures include the following arrangement of the variables:

1. wT Top Panel in Figure 18
2. -uw
3. w
4. u
5. η Bottom Panel in Figure 18

A. RESULTS FOR 19 AUGUST

This period was from 1226 to 1244 CST. Measurements in the air were made at 1.5 and 4.0 meters above mean water level. Higher waves existed in this period than during the other period considered, 26 September. The following descriptions for general conditions were given by Davidson (1970):

> "The weather map for 0700 and the hourly wind and wave histories for the day appear in Figure 12 (of the present study). A warm front had previously passed over southern Lake Michigan earlier in the morning. As a result of this frontal passage the winds were southerly and the atmospheric stratification was stable. The temperature difference between the 4.0 meter level and the surface was 1.2 C to 1.5 C. From mid-morning to late afternoon, there were scattered clouds. Wind (at the 16 meter level) and wave histories ($H_{1/3}$ cm, hourly averages) indicate that the waves began to develop under the influence of the steady south wind following frontal passage. Even though the wind increased during the day, the wave field appears to have obtained equilibrium by mid-morning (0900) and remained so throughout the observation period. The wind direction and wave propagation direction were observed to coincide.
>
> Figure 13 shows wind (2 and 8 meters), temperature (degrees Kelvin), and wave ($H_{1/3}$) conditions for the observational period. During the period there was a slight increase in wind speed but the wave field appears to have decreased during the last half of the period. The dynamics of the matched layer should have had no influence on the results because the critical level was effectively at infinity."

Variance and covariance spectra for this period, obtained by Davidson (1970), appear in Figure 14. Velocity variance and covariance spectra for the 1.5 meter and 4.0 meter levels appear on sides A and B respectively. The wave spectrum, along with the bandpass filter (dashed line), appears on both sides in order to relate the wave spectrum peak to extrema in the velocity spectra.

Primary features in these spectra are extrema in both variance and covariance spectra near 0.2 Hz, the wave spectrum peak. These occur for both levels. Energy maxima appear near this frequency in the variance

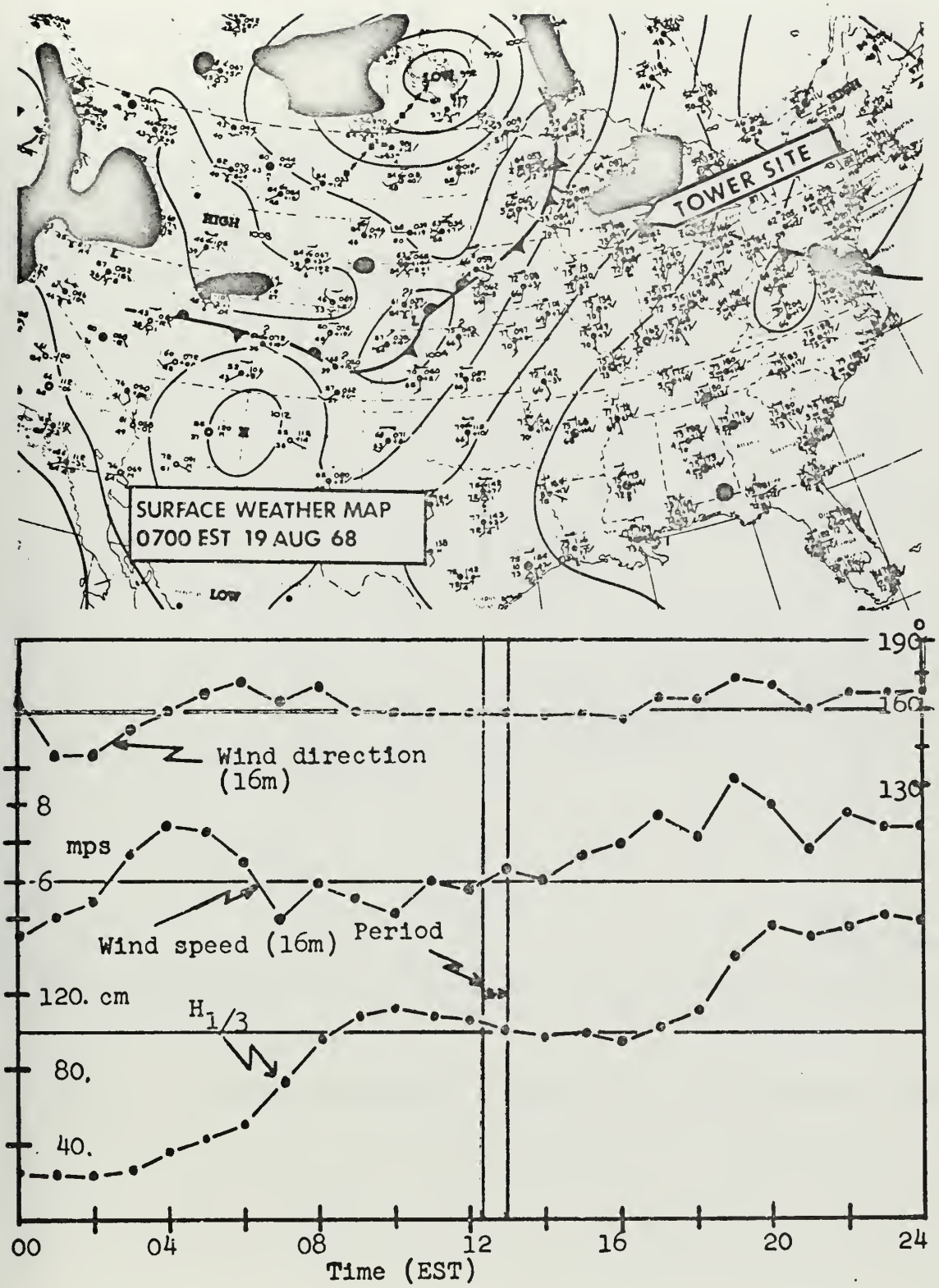

FIGURE 12. General Conditions for 19 August 1968

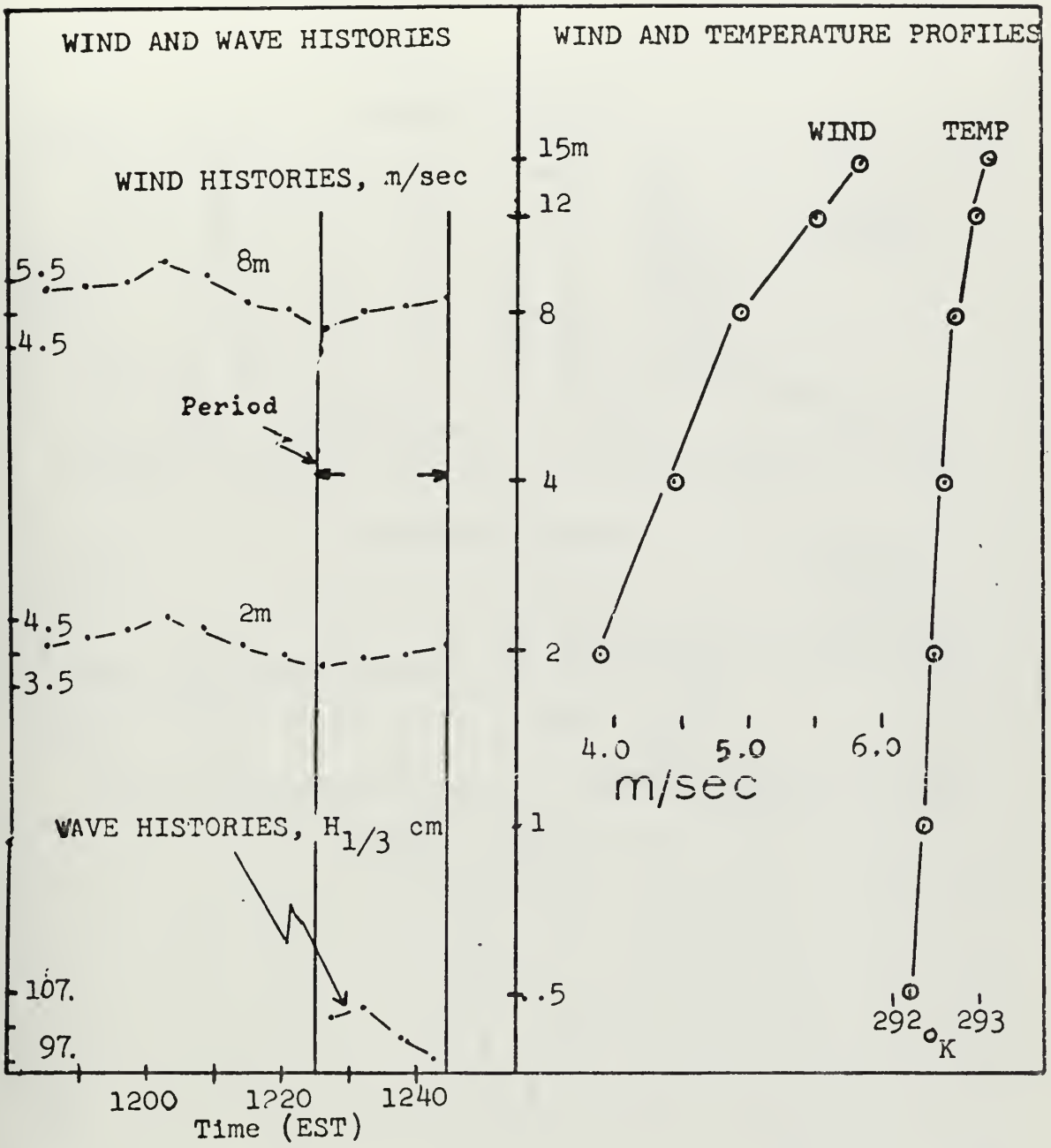

FIGURE 13. General Conditions for 1226 to 1244 CST, 19 August 1968

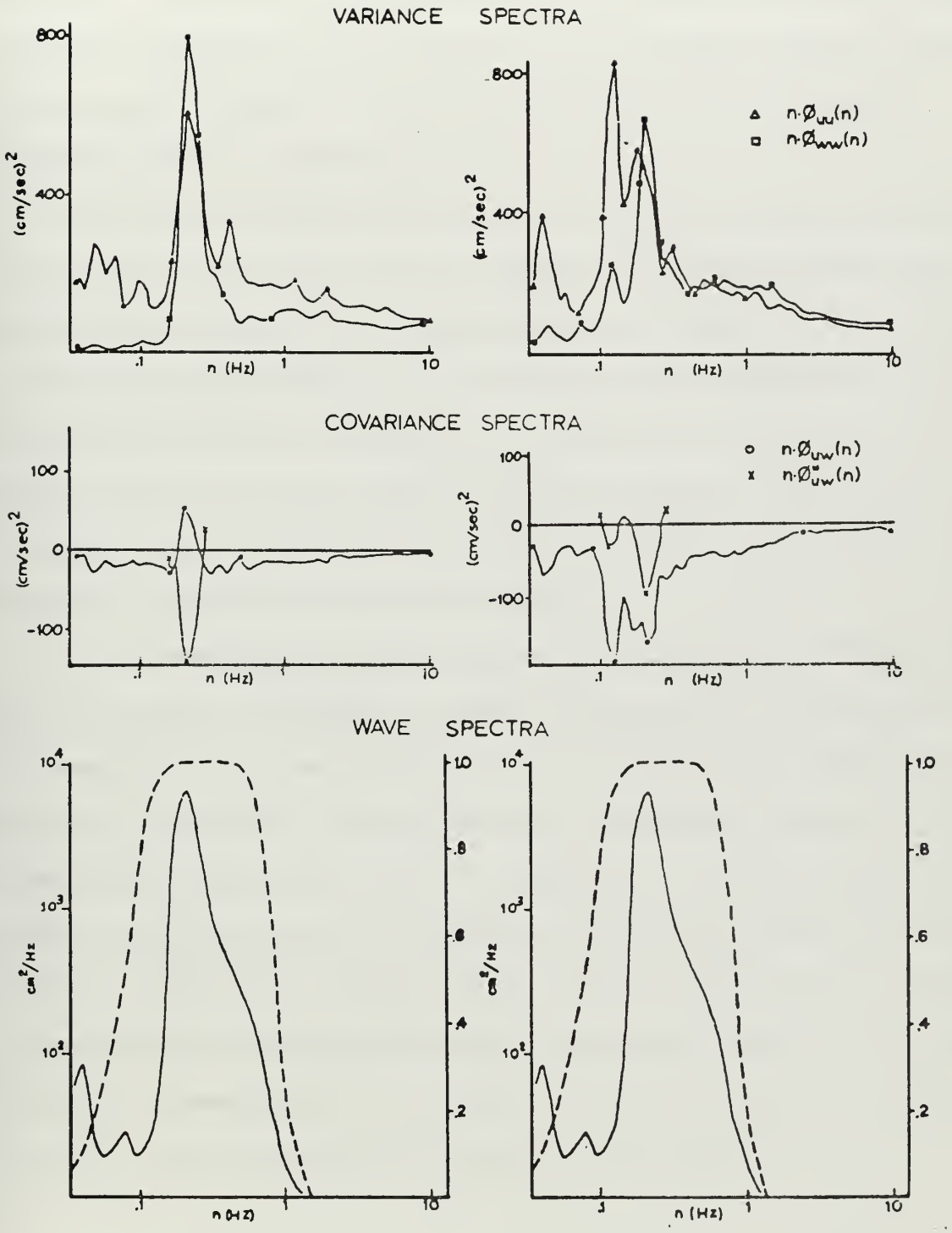

FIGURE 14. Velocity Variance and Covariance Results and Wave Spectra (With Bandpass Filter Superimposed) for 19 August 1968, With 1.5 Meter Level on the Left and 4.0 Meter Level on the Right

spectra of both components at both levels near or centered on this frequency. Covariance spectrum extrema for 1.5 meters indicate an upward transfer of momentum, $\phi_{uw}(n)>0$, and that for 4.0 meters indicate relatively larger negative values for $\phi_{uw}(n)$, resulting in, perhaps, enhanced downward transfer of momentum.

Because these results were obtained at a fixed level above mean water level, energy concentrations at the frequency of the wave spectrum peak could reflect simple bending of streamlines, as depicted in Figure 15A, in a coordinate system moving at the speed of the surface wave. In this realization, observed fluctuations in u and w would occur as shown in Figure 15B and correspond to those observed in potential flow. Referring to Figure 15B, u and w are in quadrature, 90° out of phase, and would not contribute to the shear-induced momentum flux.

In the following paragraphs, properties of the wave-induced motion in the airflow will be examined in order to determine why contributions to the momentum transfer were observed and why opposite contributions were observed at two levels along a plumb line. Comparable relations for a linear process, shown in Figure 15, suggest that the observed spectral results are due to non-linear properties of the wave-induced fluctuation within the shear flow. Dynamics of the critical level were not a factor in the results for this period because the critical level was well above the level of measurements, i.e., the base speed of 0.2Hz wave is equal to 7 m sec^{-1} and the windspeed at 4.0 meters was 5 m sec^{-1}.

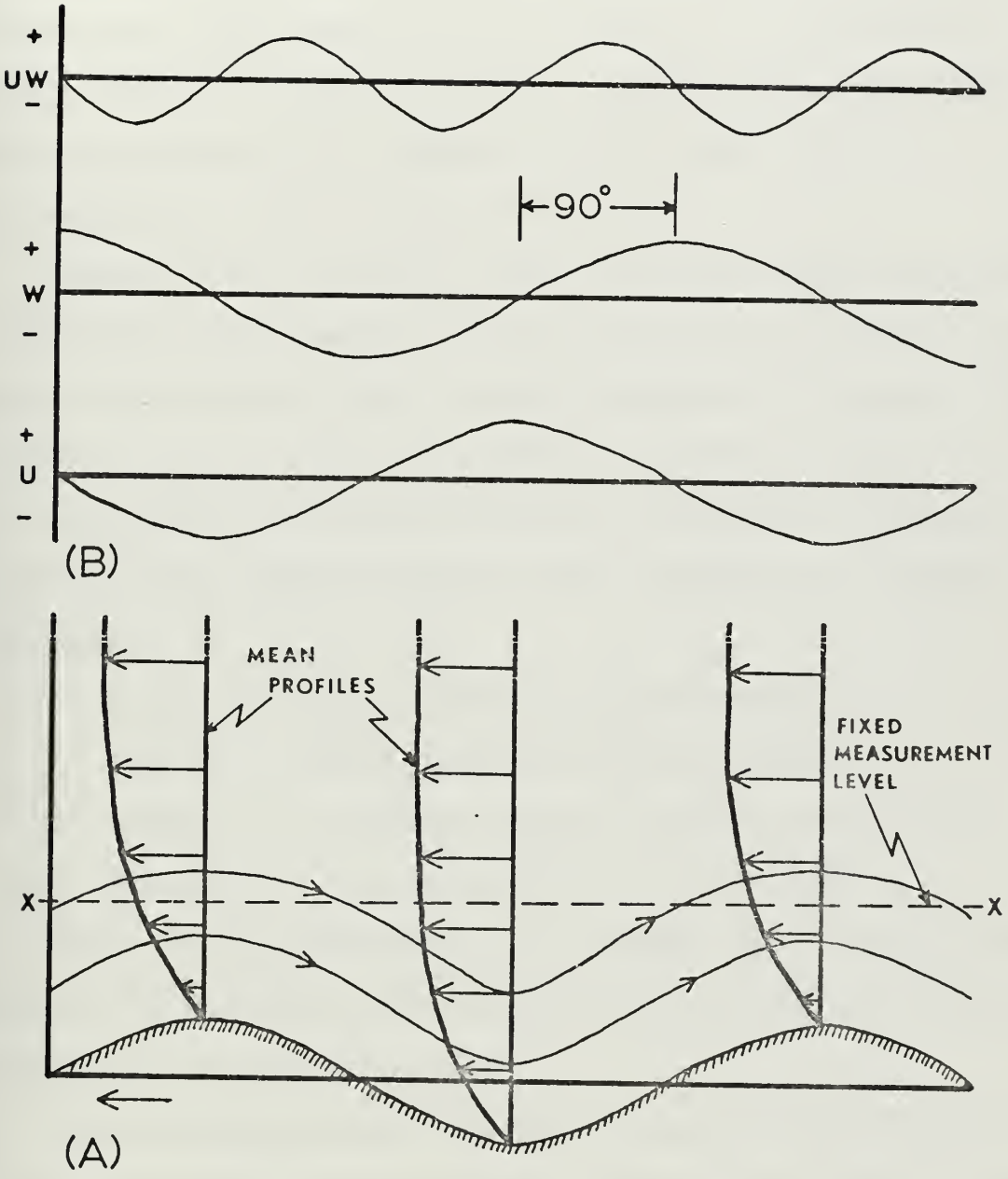

FIGURE 15. Streamlines for Potential Flow; (A) Simple Bending of Streamlines, (B) Relations Between u and w in Potential Flow

JDF/CMF results for u, w, and the waves (η) appear in Figures 16 and 17 for the 1.5 and 4.0 meter levels respectively. A general comparison between plates A in these two figures reveals a significant difference between the u-w JDF contours at the two levels. U-w JDF contours at 1.5 meters, Figure 16, are close to being concentric circles while those for 4.0 meters, Figure 17, are asymmetrical with a major axis 135° counterclockwise from the positive u-axis.

Although results appearing in plate A of these figures represent, statistically, the probability of joint occurrences of fluctuations of various magnitudes of u and w, further discussion of the results will be within the context of physical processes. Therefore, these results will be interpreted from the point of view that the respective quadrants, counterclockwise from the positive u-axis, represent the following processes:

1. Quadrant I - upward transfer of positive momentum;
2. Quadrant II - upward transfer of deficit momentum;
3. Quadrant III - downward transfer of deficit momentum; and
4. Quadrant IV - downward transfer of positive momentum.

Herein, negative fluctuations in u represent deficit momentum and positive fluctuations represent positive momentum relative to the mean momentum at the observation level.

General patterns occurring in plate A agree with those physical processes interpreted from the cospectral results. The 1.5 meter cospectrum, with the band defined by the bandpass filter, indicated that, in the mean, there was a reduction in the net downward transfer of momentum. The reason for this (Figure 16, plate A) is probably because there is a decrease in downward transfer of positive momentum (Quadrant IV) and an increase in the

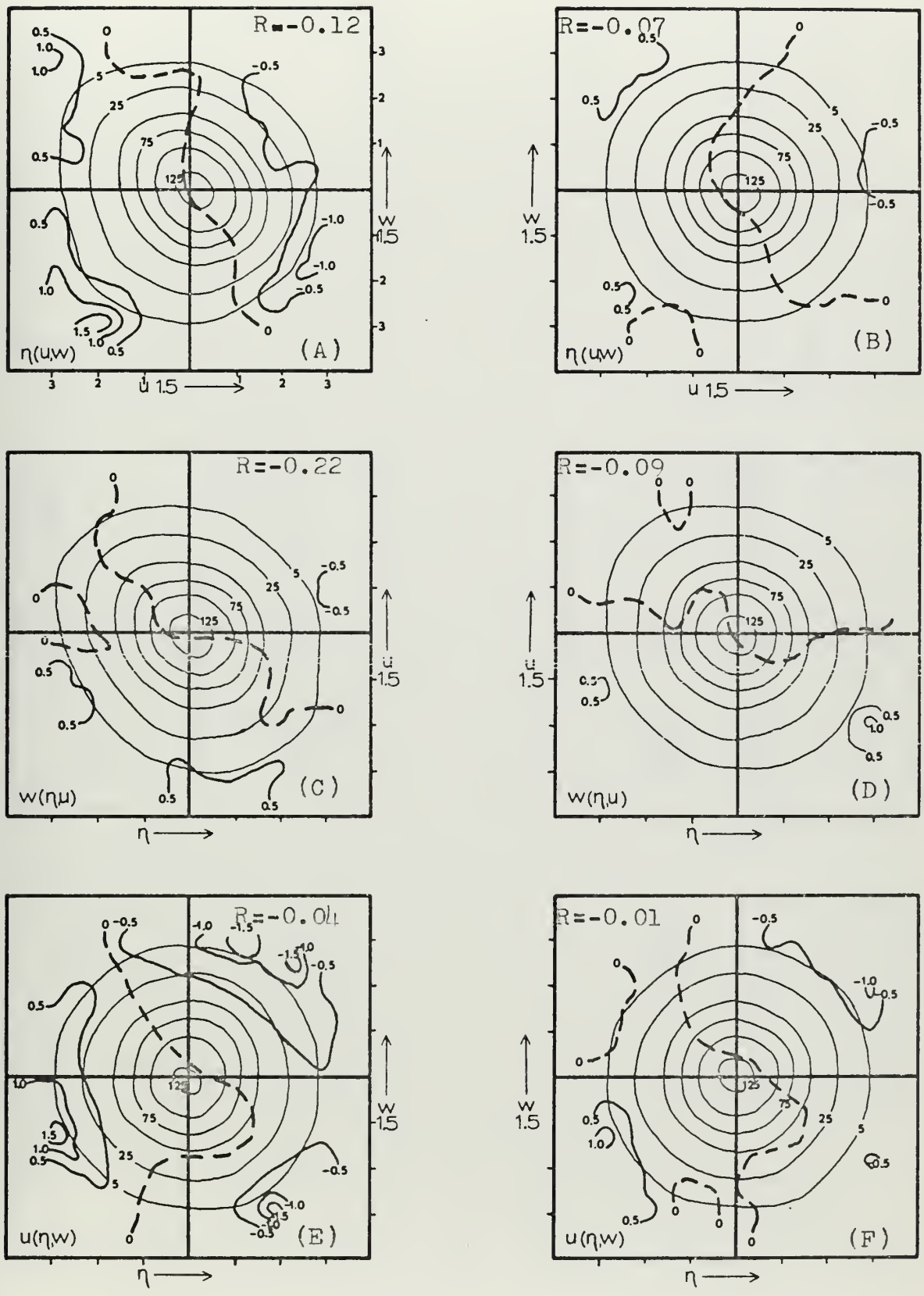

FIGURE 16. U-W JDF/CMF Results for 1.5 Meters for 19 August 1968

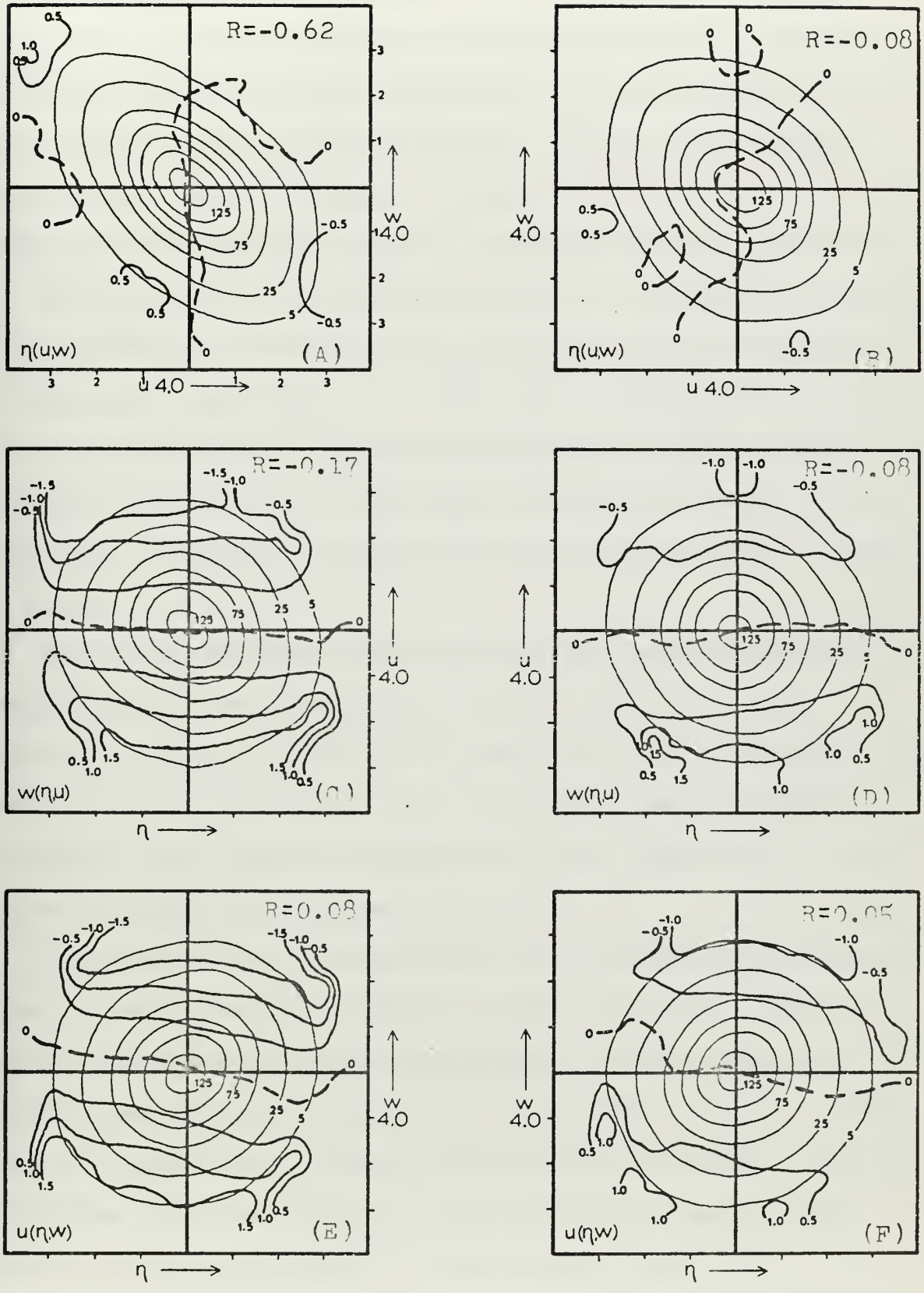

FIGURE 17. U-W JDF/CMF Results for 4.0 Meters for 19 August 1968

downward transfer of deficit momentum (Quadrant III). The cospectrum (Figure 14) for the 4.0 meter level represented enhanced net downward transfer of momentum. This is complemented by the JDF results in which the probability contours are asymmetrical, elliptical, and represent significantly greater probability for upward transfer of deficit momentum (Quadrant II) and downward transfer of positive momentum (Quadrant IV).

For the 1.5 meter level slight asymmetry of low probability contours are indicative of greater than normal occurrences of larger negative fluctuations in u at this level. These large negative fluctuations in u do not appear to have a preferred association with either positive or negative fluctuations in w. The latter interpretation follows from the fact that the probability contours have a flat edge appearance at negative u values.

The role of the waves in producing the above general patterns and deviations can be examined from CMF contours for the wave heights in plates A of Figures 16 and 17. The general CMF patterns agree with those expected for measurements at a fixed level within bending streamlines, potential flow. Observed fluctuations in u and w with respect to the waves for potential flow appear in Figure 15.

For potential flow, the CMF patterns for the waves would be maximum positive wave values associated with negative u and zero w. Maximum negative wave values would be associated with positive u and zero w. A sufficient deviation from the pattern is the bimodal, or split, maxima and, to a lesser extent, minima in the wave CMF distribution. There are sufficient points contributing to the split maxima to maintain this pattern even with the addition of random numbers (Figure 16B).

The statistical significance of the bimodal extrema can also be evaluated by examining the JDF's for u and the waves and w and the waves which appear in plates C and E of Figure 16. The asymmetry expected in potential flow, due to negative correlation between u and η, does not appear in plate C of this figure. There exists a very slight asymmetry along the 135° axis but it is not as large, for example, as that between uw appearing in plate A of Figure 16. In fact, the JDF for u and η are nearly as concentric as those for w and η, which in potential flow should be concentric because the two variables are 90° out of phase.

Probable causes for the deviations in both JDF and CMF results, from that predicted by potential flow theory, will be examined from phase-amplitude results. Phase-amplitude relations for the variables u, w, T, -uw, and wT with respect to the wave appear in Figures 18 and 19 for the 1.5 and 4.0 meter levels respectively. As previously indicated each figure has three panels which represent:

1. small waves (A) - waves less than 1.5σ;
2. large waves (B) - waves greater than 1.5σ; and
3. all waves (C).

In Figure 18 the wave appears to be a near perfect sine function but the traces for u and w are distorted. Distortion in u and w are most evident within the negative fluctuation of each. In general, at both levels, extrema in w occur over the node being positive over the rising part of the wave and negative over the sinking part. In general, extrema in u are 180° out of phase with the wave being negative over the crest and positive over the trough.

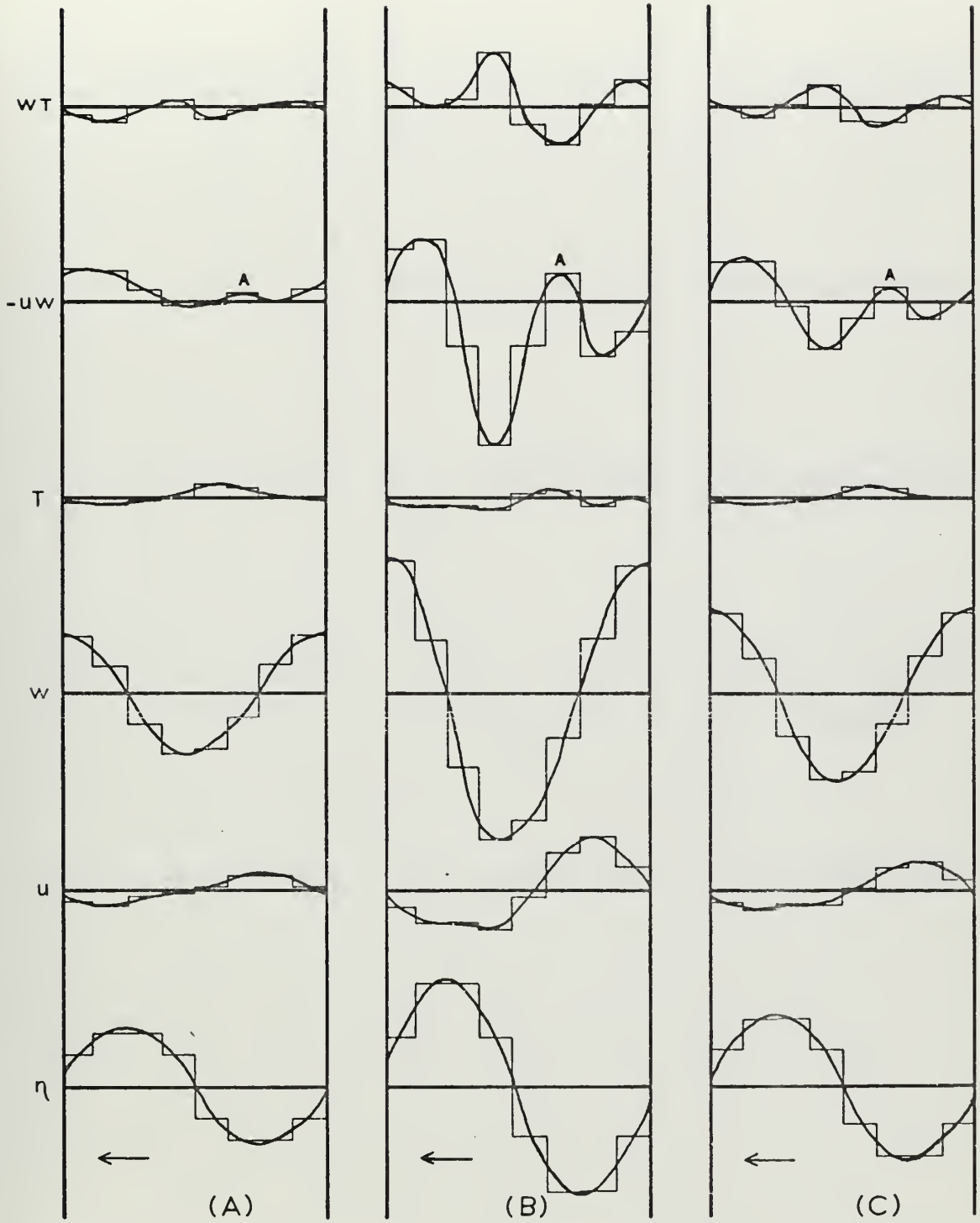

FIGURE 18. Phase-Amplitude Results for 1.5 Meters for 19 August 1968
(A) Small Waves, (B) Large Waves, (C) All Waves

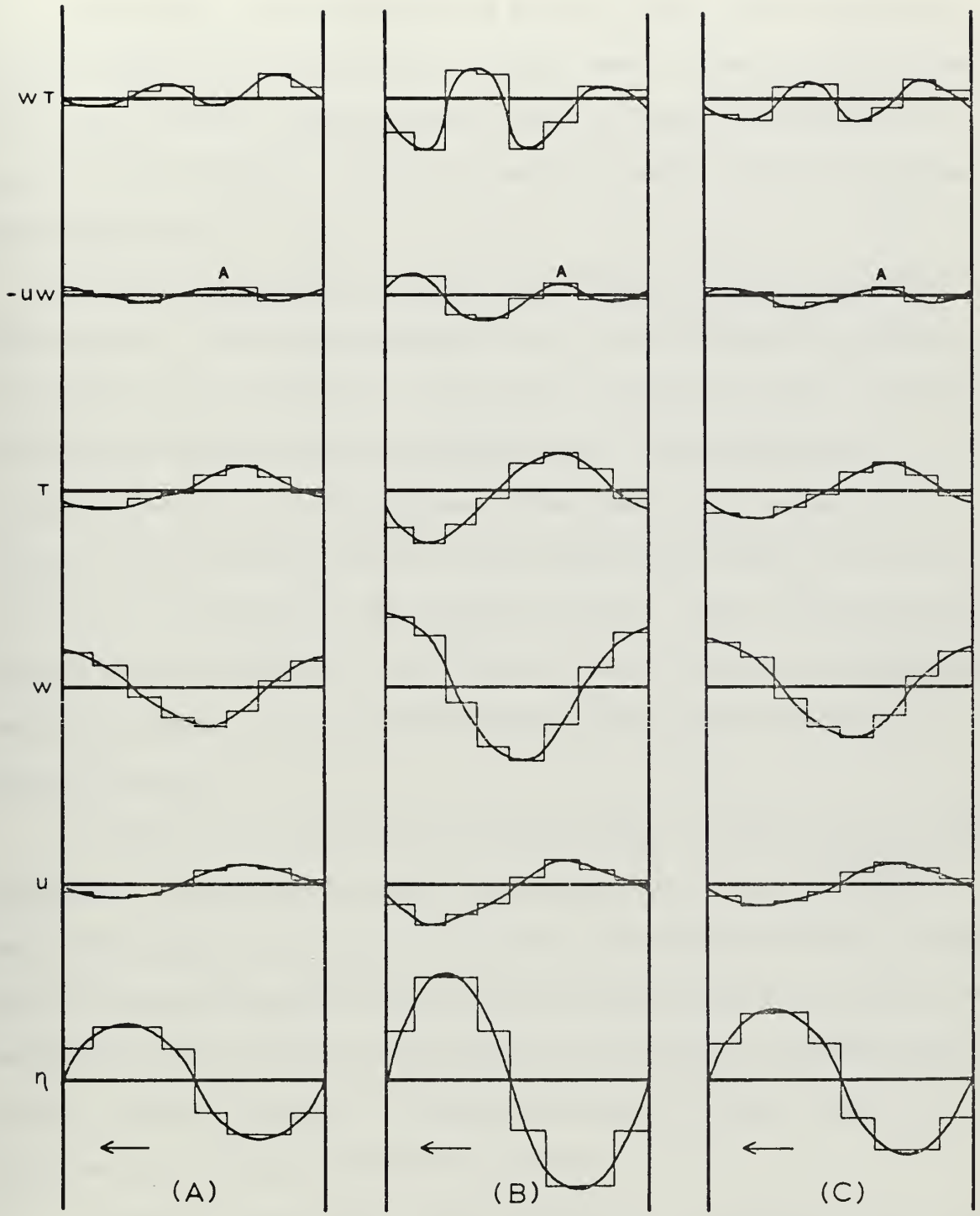

FIGURE 19. Phase-Amplitude Results for 4.0 Meters for 19 August 1968
(A) Small Waves, (B) Large Waves, (C) All Waves

A significant deviation from pure potential flow is the distortion in the u phase-amplitude for the 1.5 meter level. Negative fluctuations in u, at 1.5 meters, extend further behind the wave than predicted by potential flow theory. In fact, the maximum negative value of u occurs behind the crest.

Distortions which appear insignificant within the phase-amplitude depiction for u and w are emphasized in the -uw phase-amplitude results which will now be considered. Figure 20 is included in order to compare the observed results with those predicted by a linear expansion, i.e., Fourier series, of the fluctuations. Phase-amplitudes represented in Figure 20 were obtained with sine waves using phase angles, with respect to the wave, obtained from the spectral analysis. The resulting symmetry along the wave is evident in this figure. Also, there is a mean downward momentum transport ($-\overline{uw}>0$) when the phase relation between u and w is greater than 90°.

In comparison to the linear predictions shown in Figure 20, -uw phase-amplitudes obtained in this study were asymmetrical. The -uw phase-amplitude results, for large waves, panels B in Figures 18 and 19, reveal that the possible processes (upward and downward transfer of positive and negative momentum) are not as predicted by results from a linear description. In fact, downward transfer of positive momentum, denoted as point A, is much smaller than any of the other processes.

In summary, these results, which correspond to a case where the waves were in a state of equilibrium or slight decay, indicate that, as a first approximation, the airflow adjacent to the waves conforms to the irregular mobile wave surface. This was particularly true for the 1.5 meter level where JDF contours were nearly concentric. However, more detailed analyses

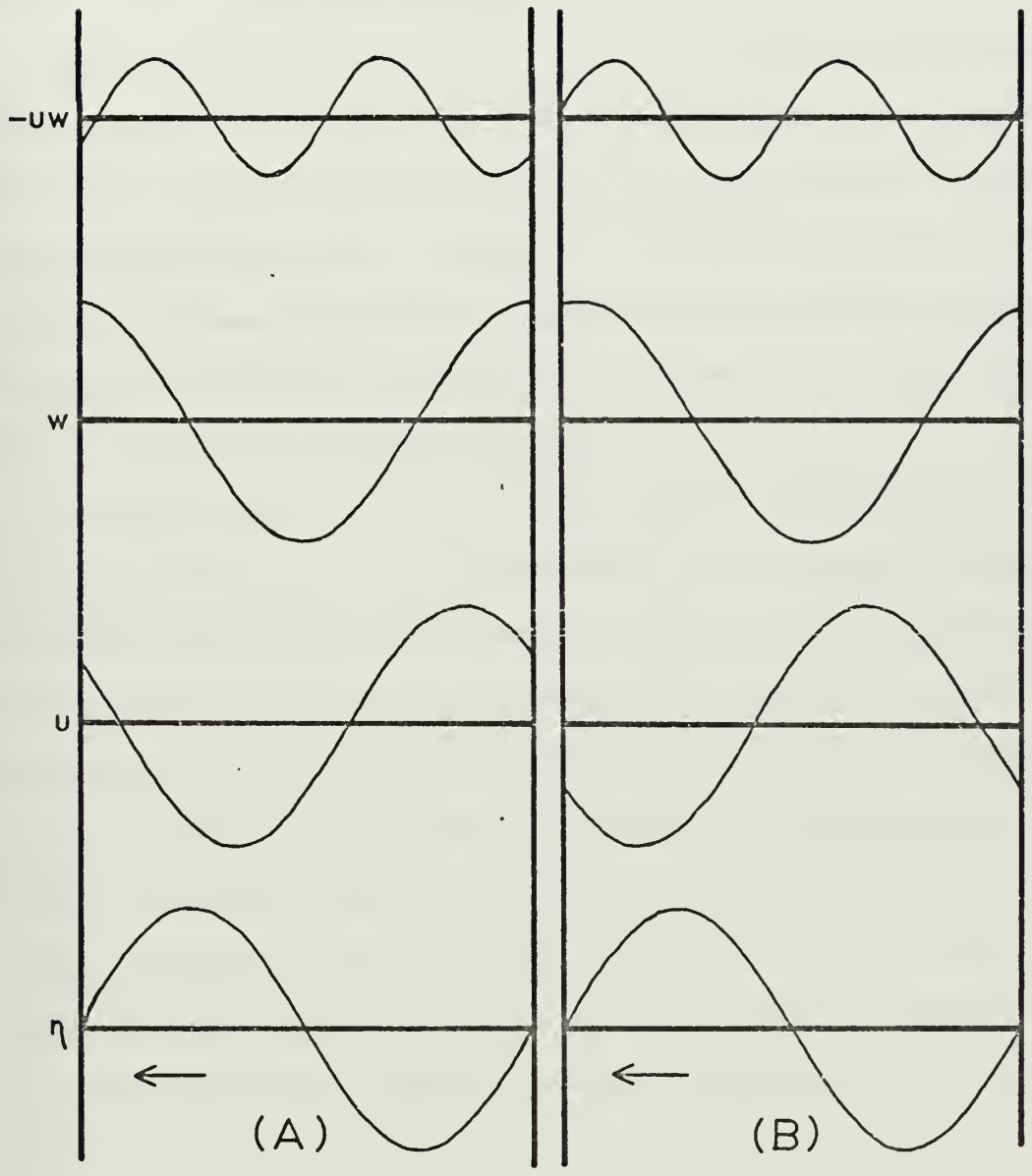

FIGURE 20. Phase-Amplitude Results for Sine Waves Utilizing Spectral Analysis Phase Angles; (A) 1.5 Meters, (B) 4.0 Meters for 19 August 1968

of JDF/CMF results and also analyses of phase-amplitude results revealed significant distortions, from the potential flow prediction, in the u component. This was not the case for the w component which exhibited, at both levels, phase relations predicted by potential flow.

Phase-amplitude results for -uw appeared to show most clearly the processes associated with a wave-induced fluctuation in the airflow. At both levels upward and downward transfer of deficit momentum appeared to be the dominant process. Therefore, assuming that random or shear-induced properties are averaged out during phase-amplitude computations, these results indicate that the waves influence did not enhance the downward transfer of positive momentum.

A probable cause for the distortion in the u component, at both levels, appears in Figure 21. It is suggested that a high pressure region, centered slightly behind the crest and propagating at the speed of the wave, produced the observed decelerations, and hence distortions, from the potential flow predictions in the u component. Such a pressure pattern coincides with the general condition of a decaying wave field. Because the pressure extrema are moving, it is apparent that this influence on the wind field is not the same as that by a stationary object. These interpretations suggest that, for this case, the drag coefficient should approximate the smooth flow case with some adjustment for the observed pressure influence.

B. RESULTS FOR 26 SEPTEMBER

This period was from 1355 to 1413 CST and the measurements were at 1.5 and 4.0 meters. Although the waves were not as high during this observation period as they were on 19 August, they increased slightly during the period. The wave spectrum was observed to have changed shape

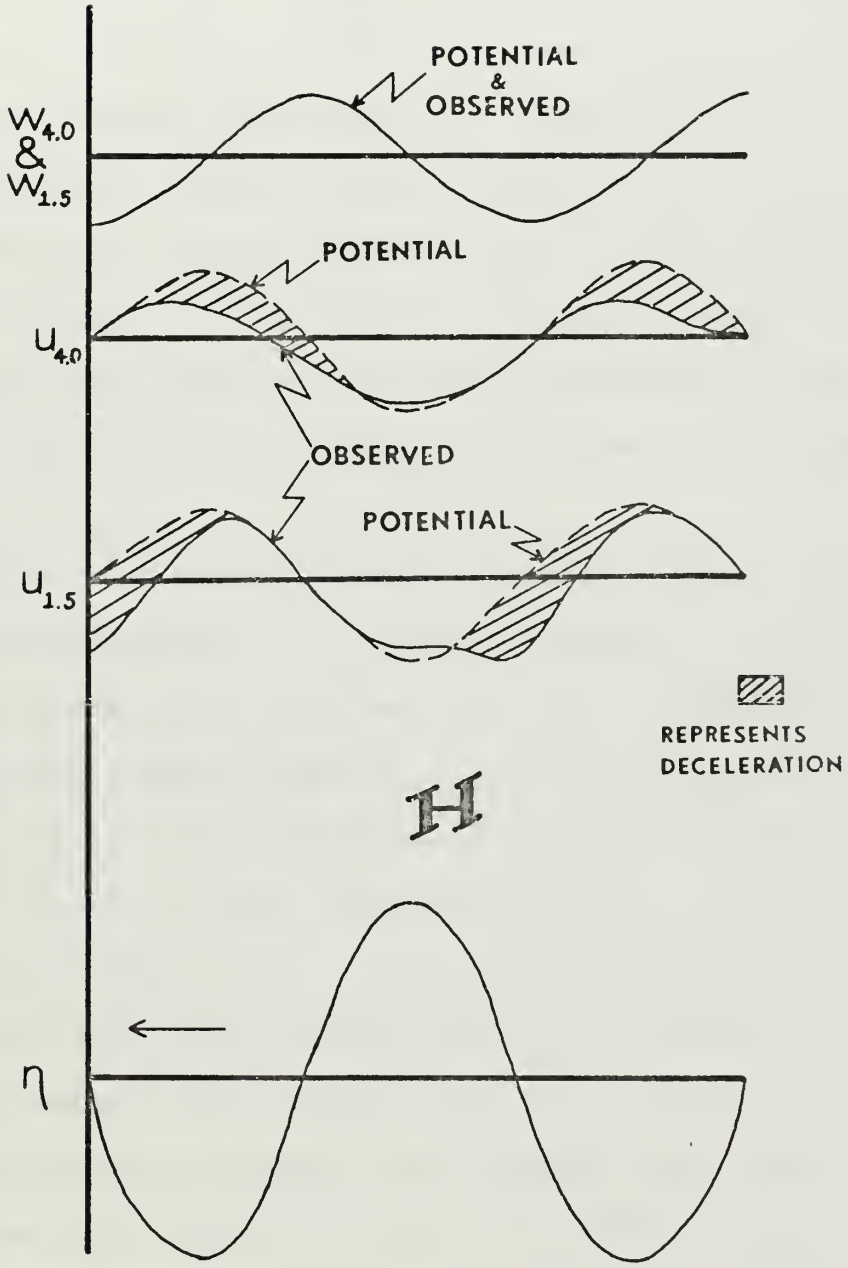

FIGURE 21. Summary Illustrating Probable Cause for the Distortion in the u Component for 19 August 1968

during the day. This change was a shift of the spectral peak to a lower frequency. The weather for the day (abridged from Davidson, 1970) is shown in Figure 22. The wind during the observation period was relatively constant and the hydrostatic conditions were unstable with the water temperature approximately 5 C higher than the air temperature at four meters. Wind and wave histories are shown in Figure 23.

Variance and covariance spectra for this period obtained by Davidson, appear in Figure 24 in which the velocity spectra for the 1.5 meter and 4.0 meter levels appear on sides A and B respectively. Again the wave spectrum peak, with the bandpass filter (dashed line), appears on both sides.

Similar to 19 August, the primary feature in these spectra are extrema in both variance and covariance spectra, at both levels, near the wave spectrum peak approximately 0.26 Hz. Covariance spectra indicate enhanced downward transfer, $\phi_{uw}(n)<0$, of momentum for both levels contrary to the 19 August spectra which showed an upward transfer of momentum at the 1.5 meter level at 0.2 Hz.

JDF/CMF results for u, w, and η appear in Figures 25 and 26 for the 1.5 meter and 4.0 meter levels respectively. A general comparison of the two levels (plate A) reveals that they are similar. That is, the u-w JDF in both have a major axis of asymmetry approximately 135° counterclockwise from the positive u-axis. This general pattern agrees with the physical processes interpreted from the cospectral results which suggest a net downward transfer of momentum.

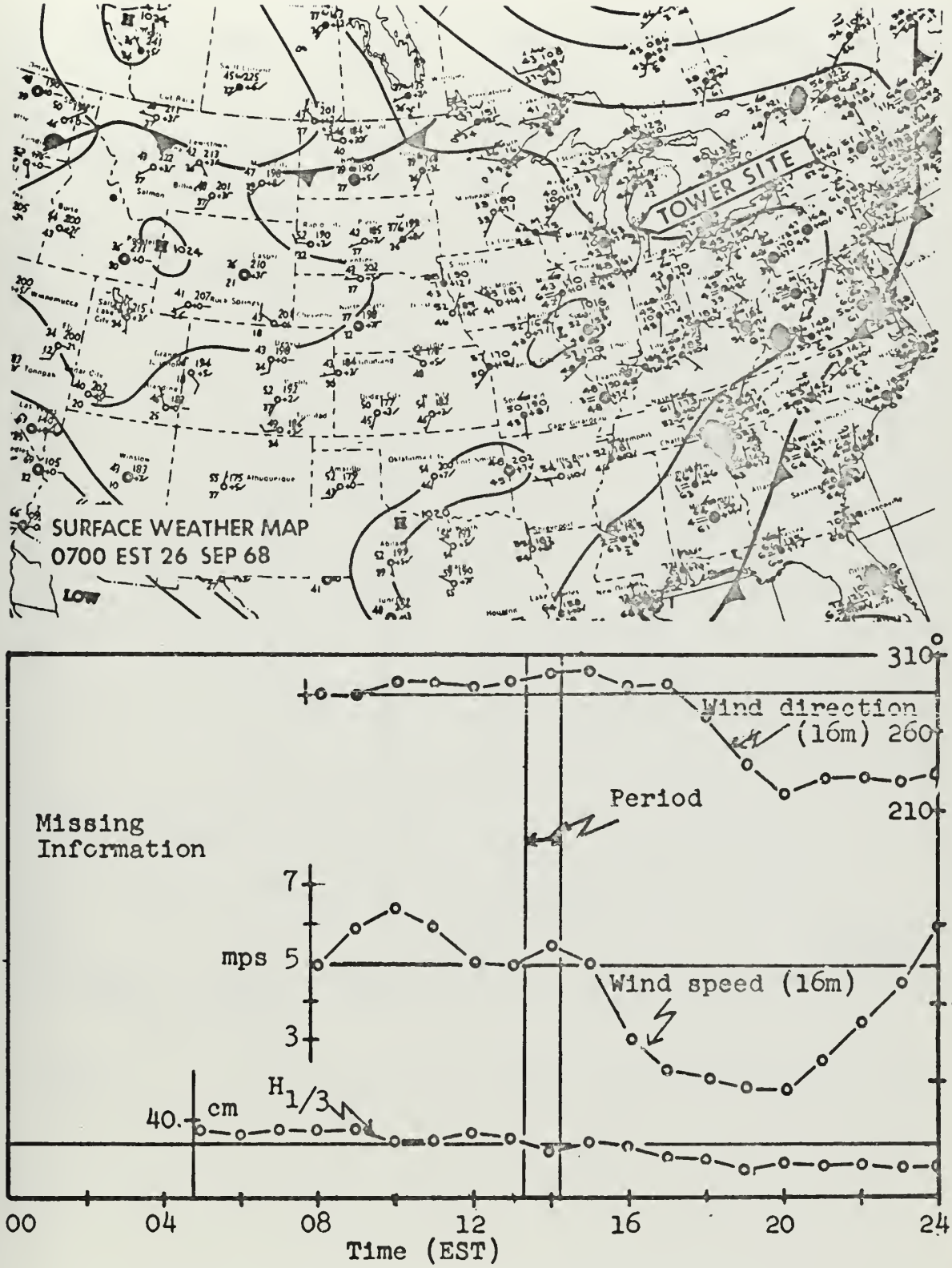

FIGURE 22. General Conditions for 26 September 1968

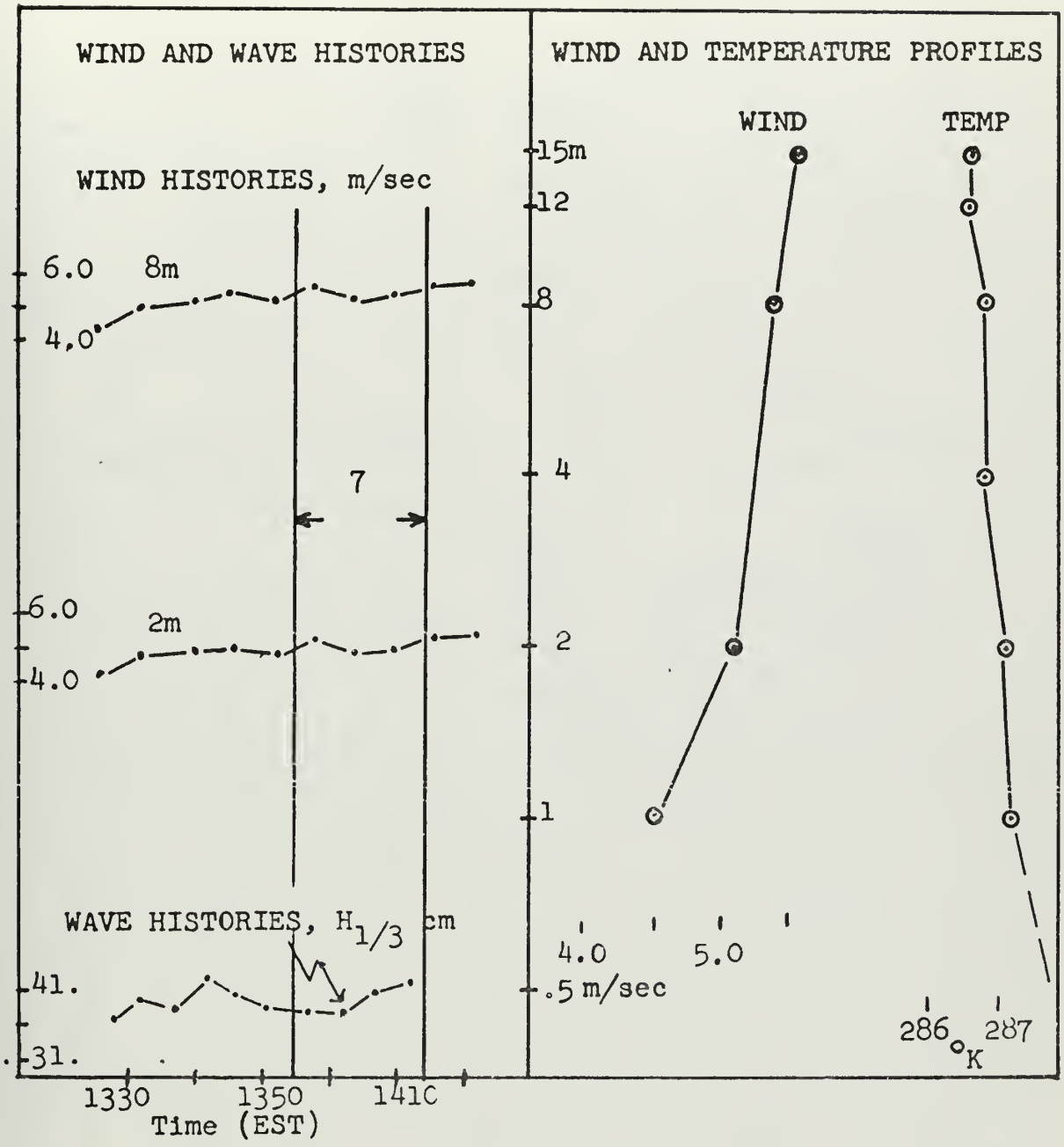

FIGURE 23. General Conditions for 1355 to 1413 CST, 26 September 1968

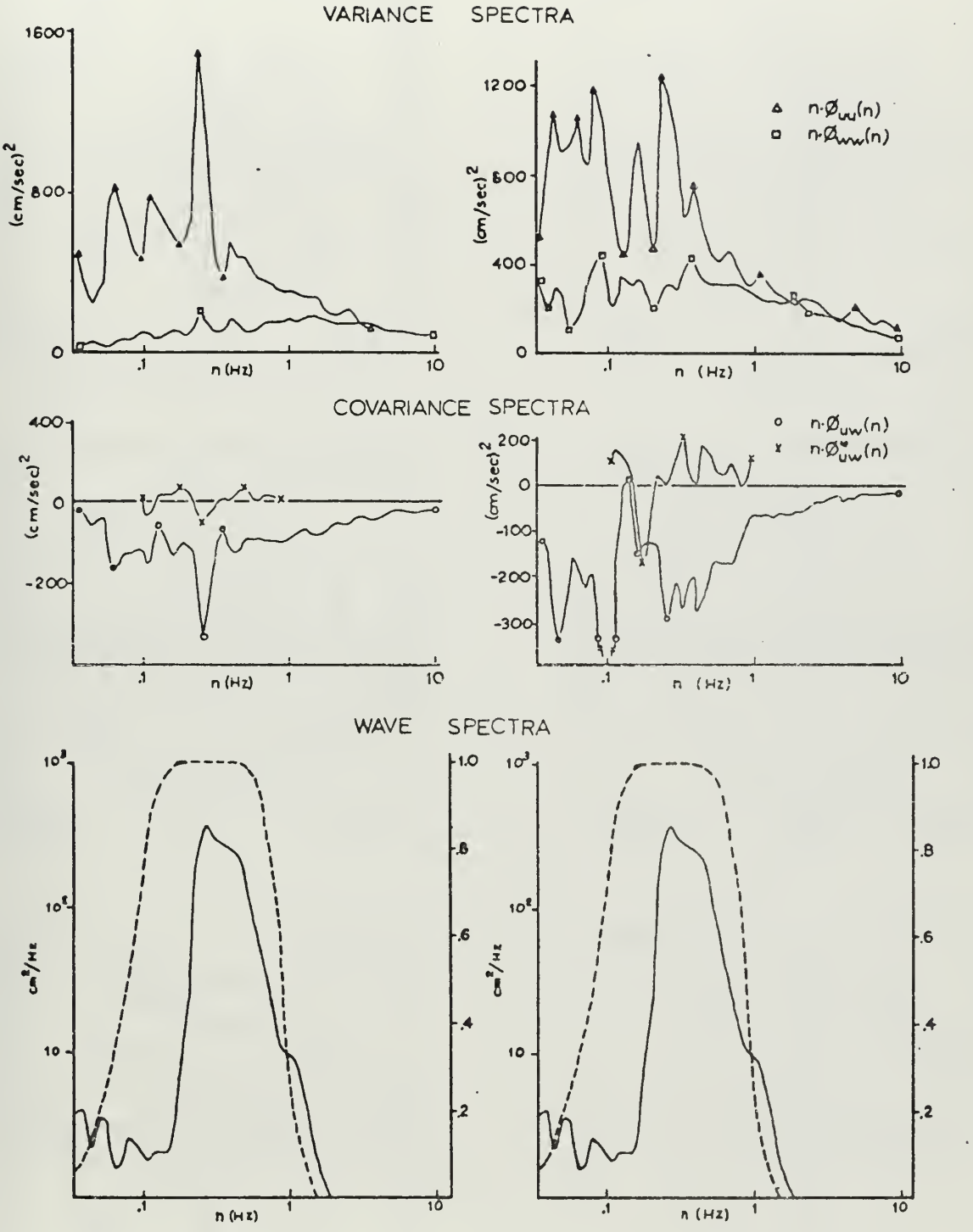

FIGURE 24. Velocity Variance and Covariance Results and Wave Spectra (with Bandpass Filter Superimposed) for 26 September 1968, with 1.5 Meter Level on the Left and 4.0 Meter Level on the Right

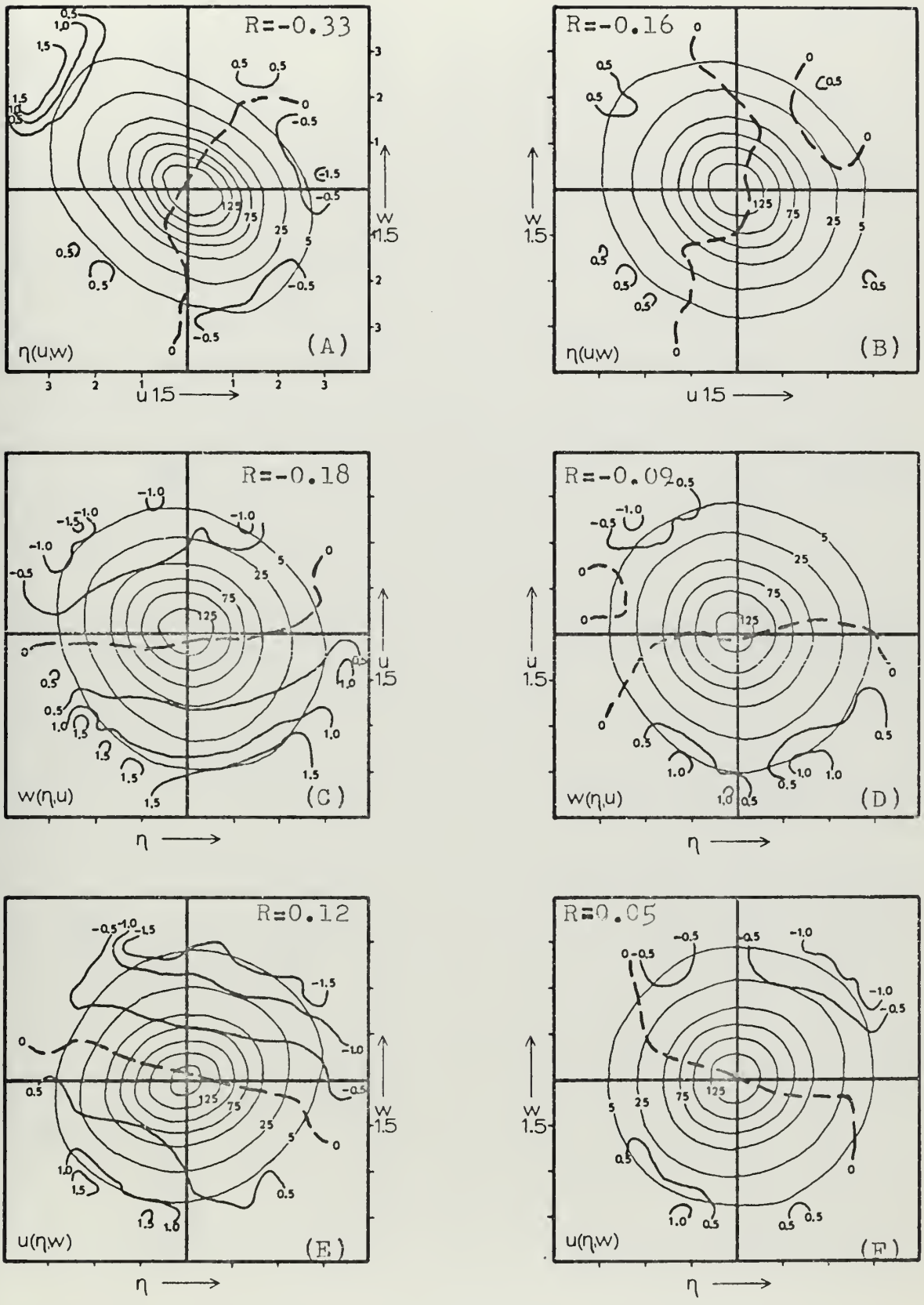

FIGURE 25. U-W JDF/CMF Results for 1.5 Meters for 26 September 1968

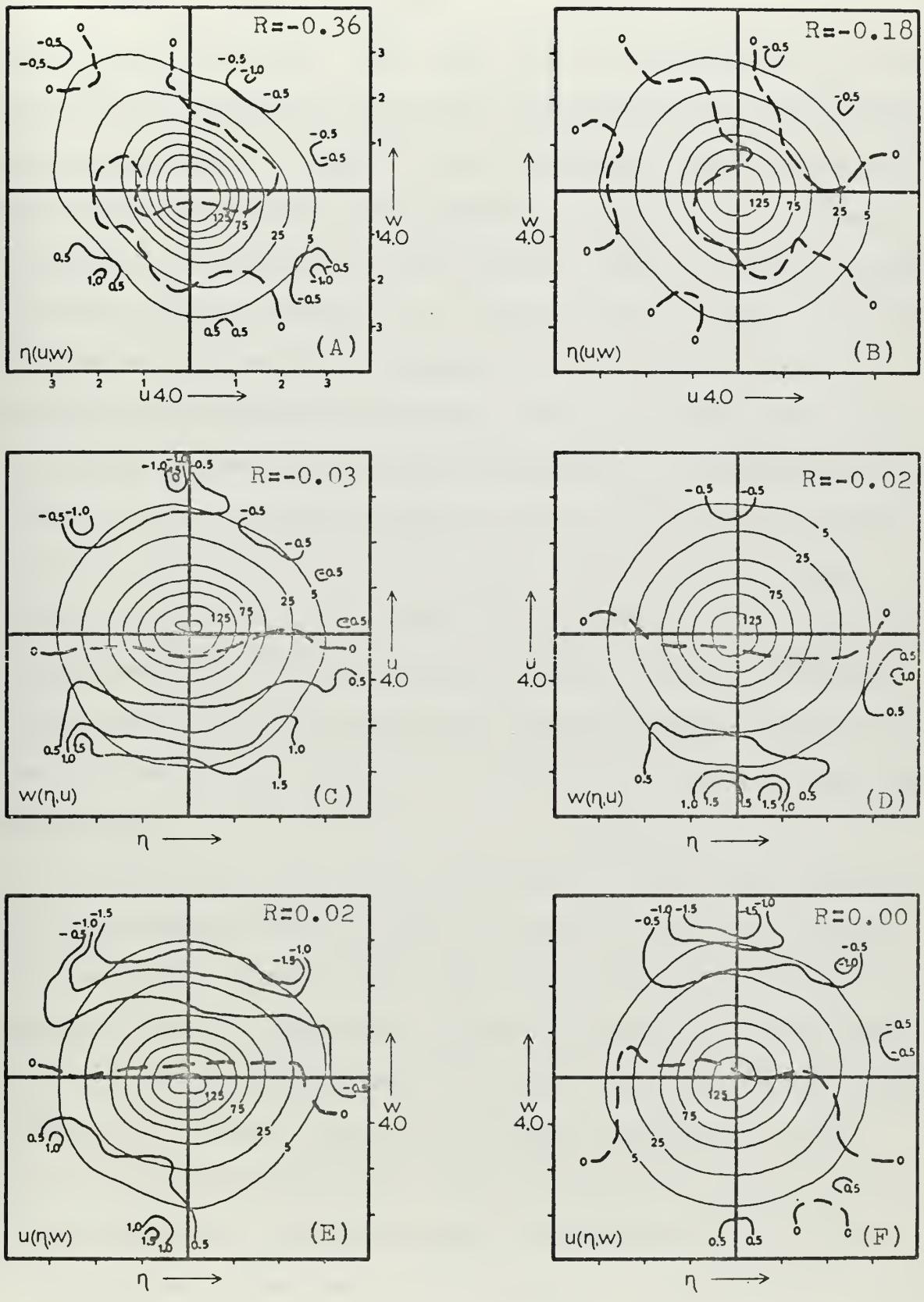

FIGURE 26. U-W JDF/CMF Results for 4.0 Meters for 26 September 1968

It would be difficult to differentiate the JDF results from those for a "normal" shear flow. In a shear flow, u-w JDF probability contours would also be asymmetrical, elliptical, and would represent significantly greater probability for upward transfer of deficit momentum (Quadrant II) and downward transfer of positive momentum (Quadrant IV). An apparent deviation is that Quadrant II and IV are not symmetric. Upward transfer of deficit momentum (Quadrant II) is the dominant of the two. Wave CMF features and phase-amplitude relations will be the primary acts in identifying the influence of the waves. At the 1.5 meter level, joint occurrences between large negative fluctuations in u and positive fluctuations in w are strongly associated with the wave crest. This relation is not as evident at the 4.0 meter level. The CMF patterns at both levels are, of course, not the same as those predicted by potential flow theory (described in the 19 August discussion). Similar to 19 August, panels C and E do not show significant asymmetries between either u or w and the waves. However, the lower level, 1.5 meters, does have the higher correlations.

The manner of the deviations from potential flow is quite apparent in the phase-amplitude results, Figures 27 and 28. Similar to 19 August, the wave appears to be a nearly perfect sine function. At both levels, u appears to have the same general relation as in potential flow, negative over the crest and positive over the trough. This relationship is almost perfect at 1.5 meters. The 4.0 meter level is distorted during the positive cycle with the maximum u shifted forward of the trough and has a flat appearance. Although, the phase of extrema in u, for 4.0 meters, is discernible in these results, the amplitude is very small and, in fact, barely above a level which would be viewed as significant.

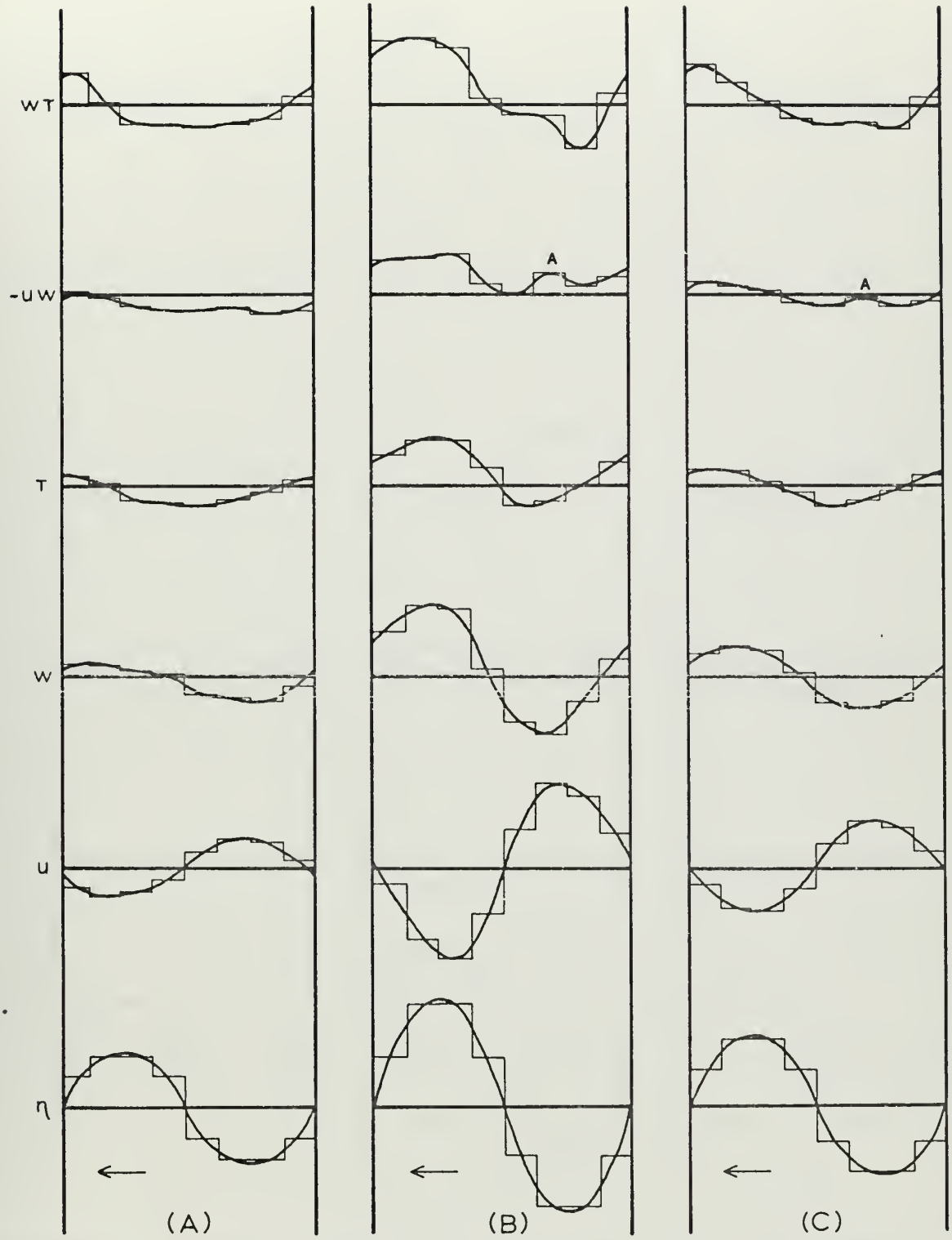

FIGURE 27. Phase-Amplitude Results for 1.5 Meters for 26 September 1968
(A) Small Waves, (B) Large Waves, (C) All Waves

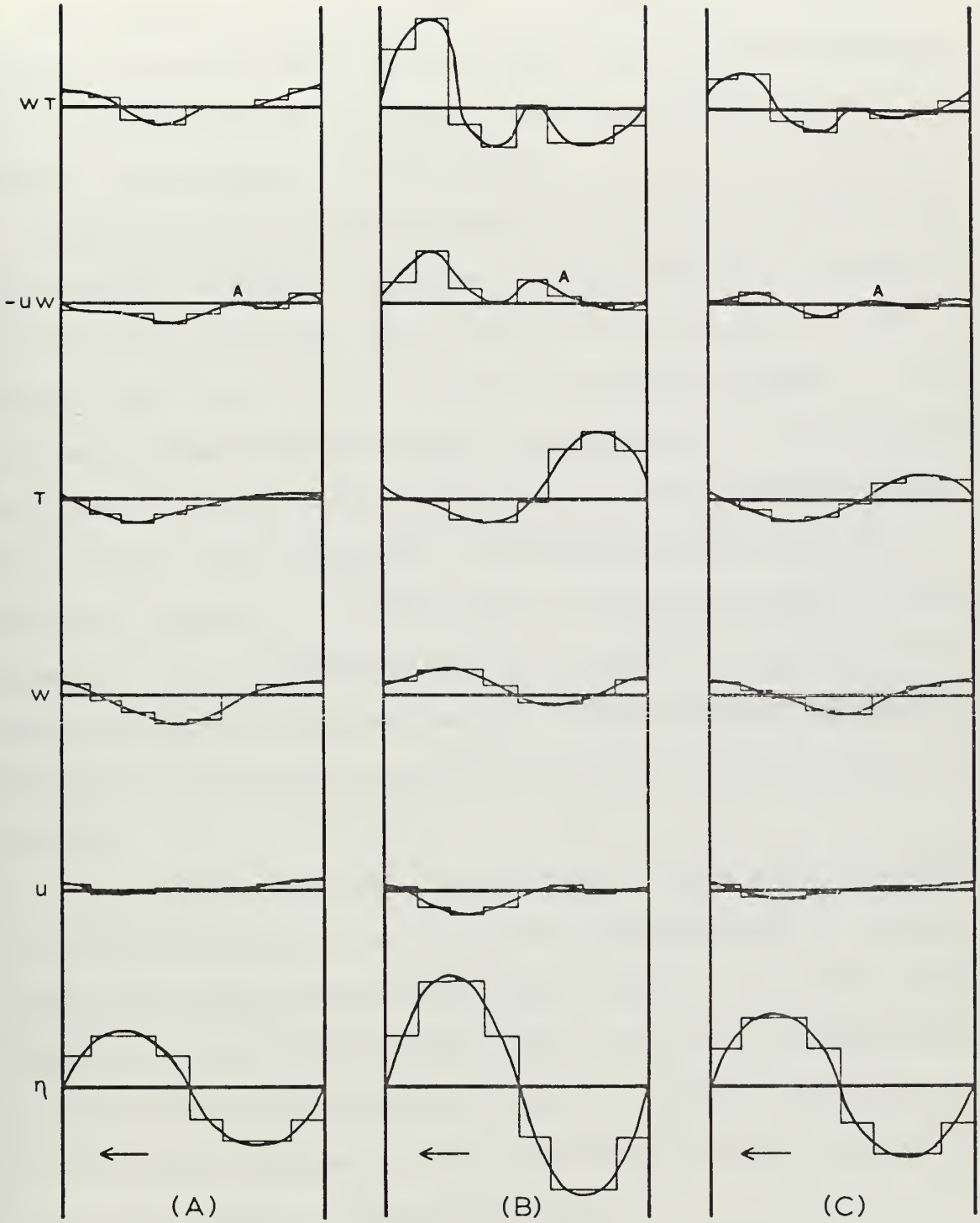

FIGURE 28. Phase-Amplitude Results for 4.0 Meters for 26 September 1968
(A) Small Waves, (B) Large Waves, (C) All Waves

The primary phase-amplitude result is the shift in the w maximum. Whereas in potential flow, and on 19 August, the w maximum is ahead of the wave crest (zero over the crest), in this observation period w maximum is directly over the wave crest.

The deviations are again emphasized in the -uw trace and Figure 29 is included for comparative purposes. Figure 29 depicts the product of two sine waves whose phase angle, with respect to the wave, are the same as u and w and which were obtained from spectral analysis. It can be seen by comparing Figure 28 and 29 that the momentum transfer processes, as depicted by JDF/CMF results, differ significantly from the results, depicted by a linear description. The dominate process (large scale waves (B) in Figures 27 and 28) appears to be upward transfer of deficit momentum and the only other process of any significance appears to be downward transfer of positive momentum. Downward transfer of positive momentum is, however, much less than the upward transfer of deficit momentum.

In summary, these results, representing a case in which the dynamics of the critical level and wave generation processes could be a factor, reveal significant differences from those observed in the other period examined. U-W JDF results for both levels indicated that upward transfer of deficit momentum and downward transfer of positive momentum were the most significant processes. These same results indicated that the former was the most dominant of these two processes.

Phase-amplitude results indicated that the asymmetrical, shear flow type, pattern of the u-w JDF were due to a near 180° phase difference between u and w. This phase difference existed because u maintained out-of phase relations with the wave extrema but the maxima in w shifted,

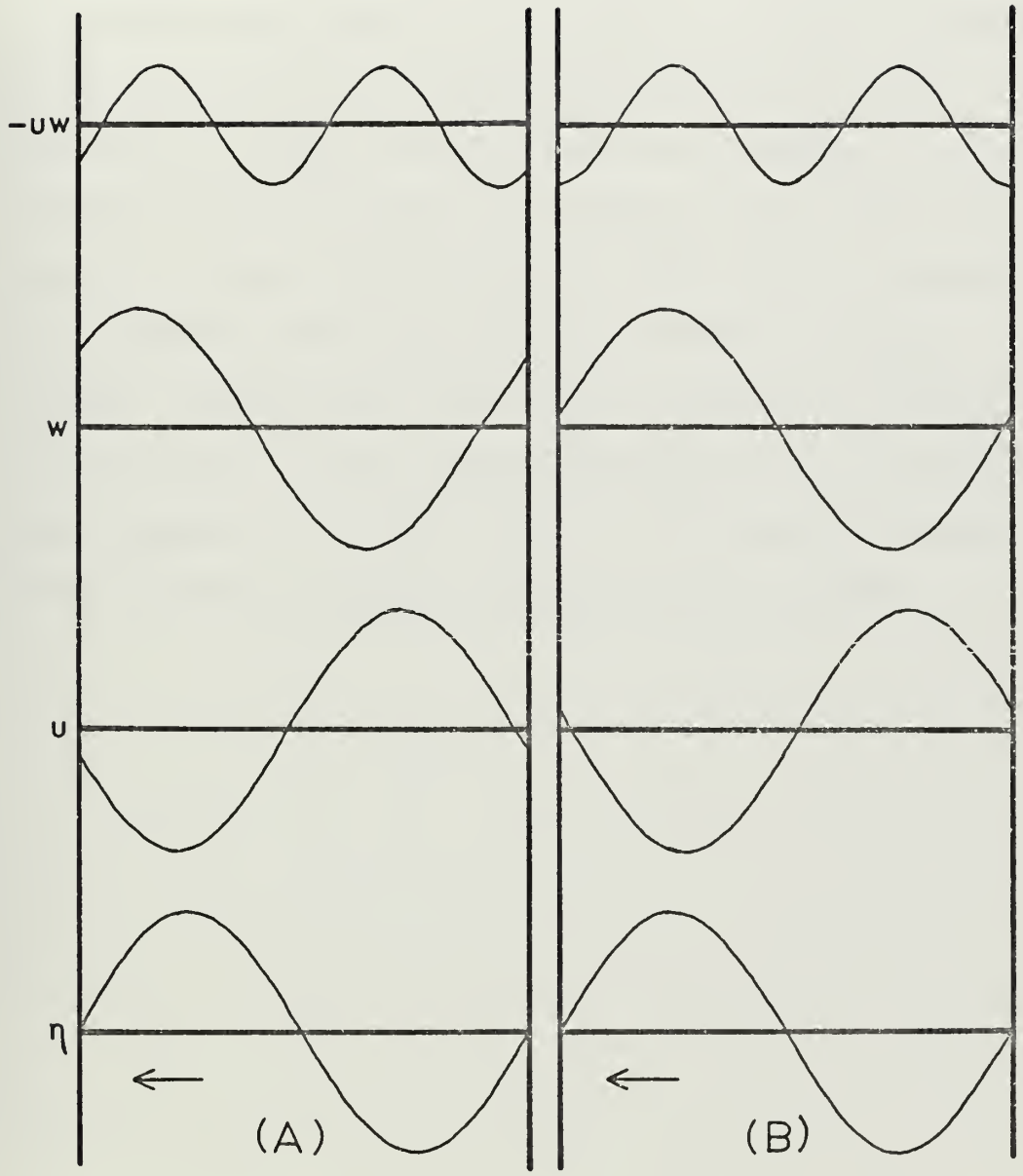

FIGURE 29. Phase-Amplitude Results for Sine Waves Utilizing Spectral Analysis Phase Angles; (A) 1.5 Meters, (B) 4.0 Meters for 26 September 1968

relative to the 19 August description, to a position over the crest. The shift in phase of the w component is predicted in the linear theory and is due to the dynamics at the critical level.

The prominence, again, of deficit momentum transfer was evident in the -uw phase relation. A physical interpretation for this, as was possible for 19 August, has not been achieved. However, it could be related to the slight distortions in both the u and w phase-amplitude traces. It is known that distortions of this type are associated, in a linear expansion, with super-position of different harmonics. It is, therefore, suggested that in this case the distortions were due to a coupling between the wave-induced fluctuations and a fluctuation of a higher frequency. The latter could be due to buoyant processes which existed over this relatively warm undulating wave surface.

V. CONCLUSIONS

In this study, turbulence data obtained over waves were examined to obtain some understanding of properties and influence of wave-induced fluctuations on the turbulent regime. Statistical procedures were used which enabled interpretations to be made on non-linear properties of the wave-induced fluctuations and on separate modes of momentum transfer. Two data periods, representing decaying and generating wave conditions, were examined and the results revealed significant difference in these two periods. The usefulness of the selected statistical procedures is supported by the following conclusions from the results of each of these two periods.

For a case when the near surface wind speed is much less than the speed of the predominant surface wave, the critical level nearly at infinity, these results indicate:

1. The primary feature of the flow is one of simple streamline bending in which the airflow conforms to the wave surface and this can be observed as high as 4.0 meters above mean water level.

2. There is a slight deceleration in the airflow due to a pressure maximum located near the wave crest. Because this pressure maximum is traveling at the speed of the wave it does not represent an obstacle to airflow as a stationary object would.

3. An observed increase in the negative correlation between horizontal and vertical components, which is normally considered to represent enhanced downward transport of positive momentum, was due to enhanced upward transfer of deficit momentum.

4. If these results are representative of conditions when the waves are in equilibrium with the wind field, an appropriate drag coefficient would be one reflecting smooth flow conditions. This is based on the fact that the airflow simply follows the wave.

For a case where the near surface wind speed and the phase speed of the predominant surface waves are about the same, the critical level near the level of the observations, the results indicate that:

1. There is an increased negative correlation between u and w that is due to a 90° phase shift of the wave-induced w component. This shift is predicted by a linear theory which is based on the dynamics at the critical level.

2. There appears to be a distortion, from potential flow predictions, in the u component and this could be due to wave-induced buoyant motion.

Future research on these data and other data obtained over natural water waves should include provisions for the statistical procedure employed in this study. Wave following sensors (for example Boston, et.al., 1969, Davis, 1969) should be used in the measurements. This would remove the necessary comparisons with potential flow predictions. Relations between temperature fluctuations and the waves should be interpreted.

```
      SUBROUTINE JDFCMF (X,Y,Z,N1,N2,A,B,NP1,C1,NP2,C2)                 00001770
      DIMENSION X(N1), Y(N1), Z(N1), A(18,18,2), B(18,18,2),            00001780
     1 NP1(18,18), C1(18,18), NP2(16,16), C2(16,16)                     00001790
C                                                                       00001800
C X, Y, AND Z OF LENGTH N1: NORMALIZED INPUT VECTORS                    00001810
C II AND JJ SET LIMITS: 18 BY 18 MATRIX                                 00001820
C N2 COUNTS OBSERVATIONS WITHIN THE II BY JJ LIMITS                     00001830
C A(18 BY 18|1): 2-WAY CONTINGENCY TABLE| A(18 BY 18|2): SUMS OF 3RD    00001840
C B(18 BY 18|1): PROB PER SIGMA**2| B(18 BY 18|2): COND MEAN FUNCTION   00001850
C                                                                       00001860
      DO 18 K = 1,2                                                     00001870
      DO 18 J = 1,18                                                    00001880
      DO 18 I = 1,18                                                    00001890
      A(I,J,K) = 0.0                                                    00001900
      B(I,J,K) = 0.                                                     00001910
18    CONTINUE                                                          00001920
      N2 = 0                                                            00001930
      DO 20 K = 1,N1                                                    00001940
      XJJ = 2.*X(K) + 10.                                               00001950
      XII = 2.*Y(K) + 10.0                                              00001960
      JJ=XJJ                                                            00001970
      II=XII                                                            00001980
      IF ( II .LT. 1 ) GO TO 20                                         00001990
      IF ( II .GT. 18 ) GO TO 20                                        00002000
      IF ( JJ .LT. 1 ) GO TO 20                                         00002010
      IF ( JJ .GT. 18 ) GO TO 20                                        00002020
      N2 = N2 + 1                                                       00002030
      A(II,JJ,1) = A(II,JJ,1) + 1.0                                     00002040
      A(II,JJ,2) = A(II,JJ,2) + Z(K)                                    00002050
20    CONTINUE                                                          00002060
      DO 22 I = 1,18                                                    00002070
      DO 22 J = 1,18                                                    00002080
      IF (A(I,J,1) .EQ. 0.0) GO TO 22                                   00002090
      B(I,J,2) = A(I,J,2) / A(I,J,1)                                    00002100
      B(I,J,1) = A(I,J,1) *  400./N2                                    00002110
22    CONTINUE                                                          00002120
      DO 24 I = 1,18                                                    00002130
      DO 24 J = 1,18                                                    00002140
      NP1(I,J) = 10. * B(I,J,1)                                         00002150
      C1(I,J) = A(I,J,2)                                                00002160
24    CONTINUE                                                          00002170
C                                                                       00002180
C APPLY THE 9-POINT SMOOTHER                                            00002190
C                                                                       00002200
      DO 26 I = 2,17                                                    00002210
      II = I - 1                                                        00002220
```

```
      I1 = I + 1                                                                00002230
      DO 26 J = 2,17                                                            00002240
      JJ = J - 1                                                                00002250
      J1 = J + 1                                                                00002260
      D = 0.125 * (NP1(I,J1) + NP1(I,JJ) + NP1(II,J) + NP1(I1,J))               00002270
      E = 0.0625 * (NP1(II,JJ) + NP1(I1,JJ) + NP1(II,J1) + NP1(I1,J1))          00002280
      NP2(II,JJ) = D + E + 0.25*NP1(I,J)                                        00002290
      D = 0.125 * (C1(I,J1) + C1(I,JJ) + C1(II,J) + C1(I1,J))                   00002300
      E = 0.0625 * (C1(II,JJ) + C1(I1,JJ) + C1(II,J1) + C1(I1,J1))              00002310
26    C2(II,JJ) = D + E + 0.25*C1(I,J)                                          00002320
      DO 28 I = 1,16                                                            00002330
      DO 28 J = 1,16                                                            00002340
      P = NP2(I,J)*N2                                                           00002350
      IF (NP2(I,J).EQ.0) GO TO 30                                               00002360
      IF (N2.EQ.0) GO TO 30                                                     00002370
      C2(I,J) = C2(I,J)/(P/4000.0)                                              00002380
      GO TO 28                                                                  00002390
30    C2(I,J) = 0.0                                                             00002400
28    CONTINUE                                                                  00002410
      RETURN                                                                    00002420
      END                                                                       00002430
```

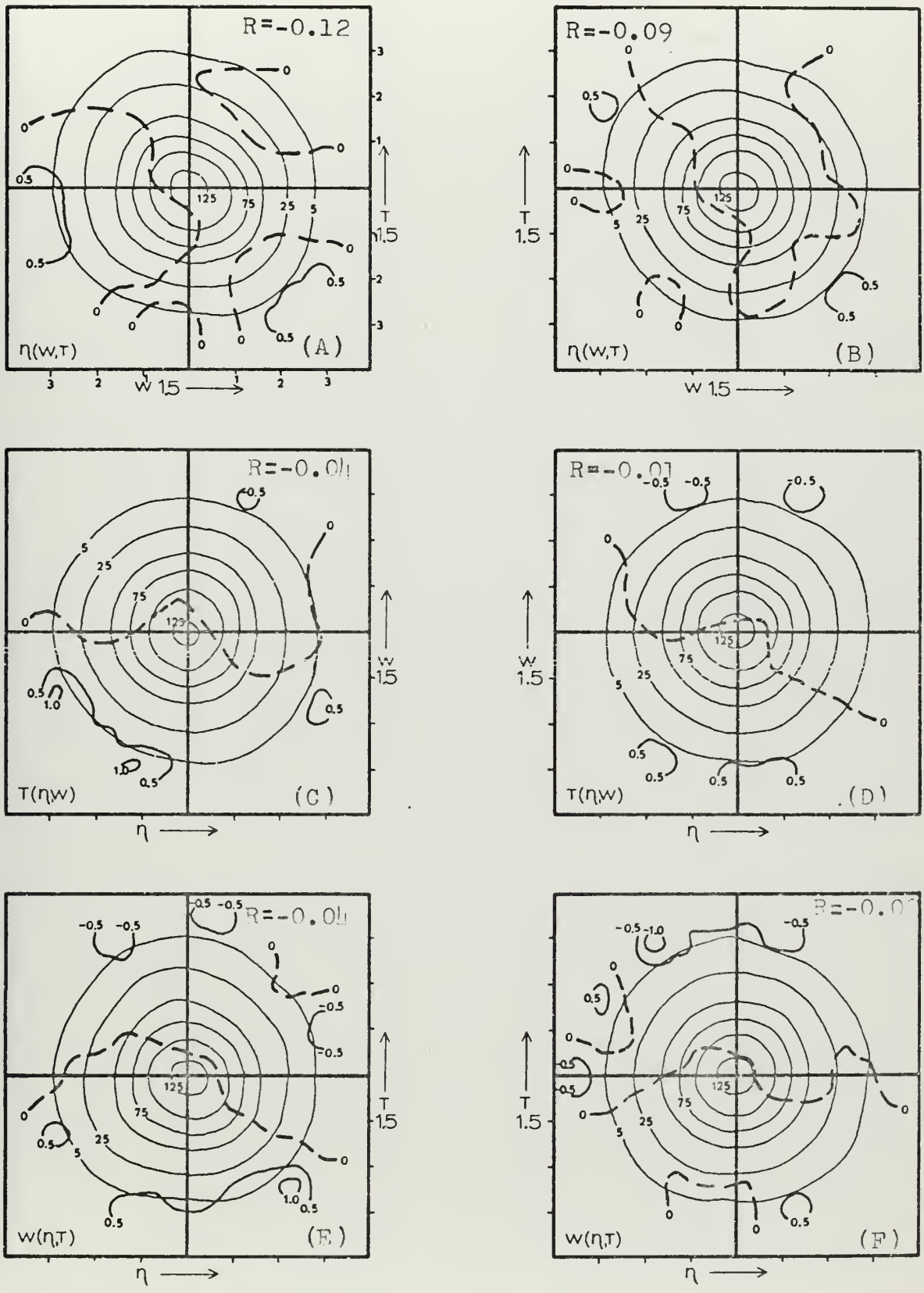

FIGURE 30. JDF/CMF Results; $W_{1.5}$ and $T_{1.5}$ with Waves for 19 August 1968.

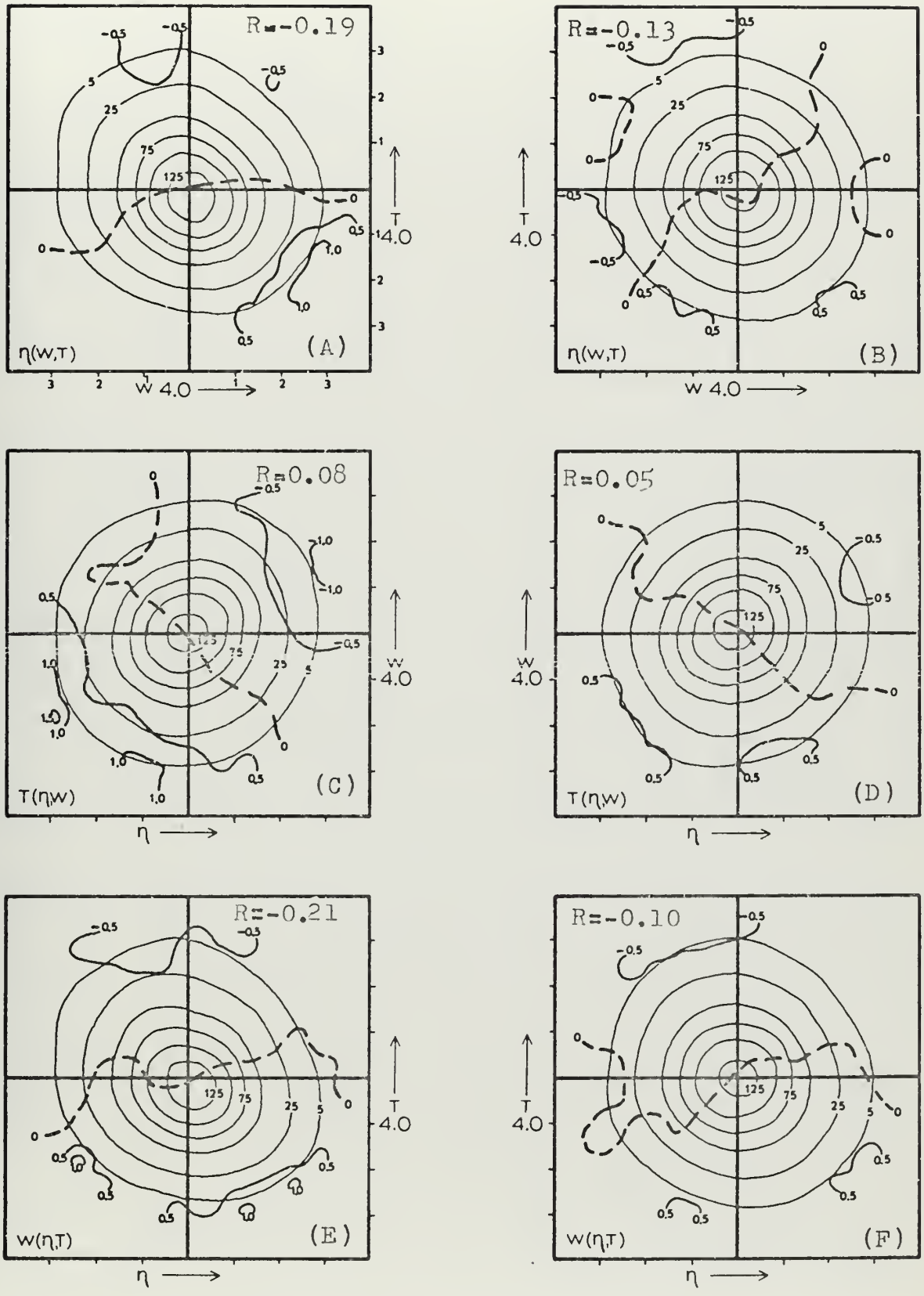

FIGURE 31. JDF/CMF Results; $W_{4.0}$ and $T_{4.0}$ with Waves for 19 August 1968.

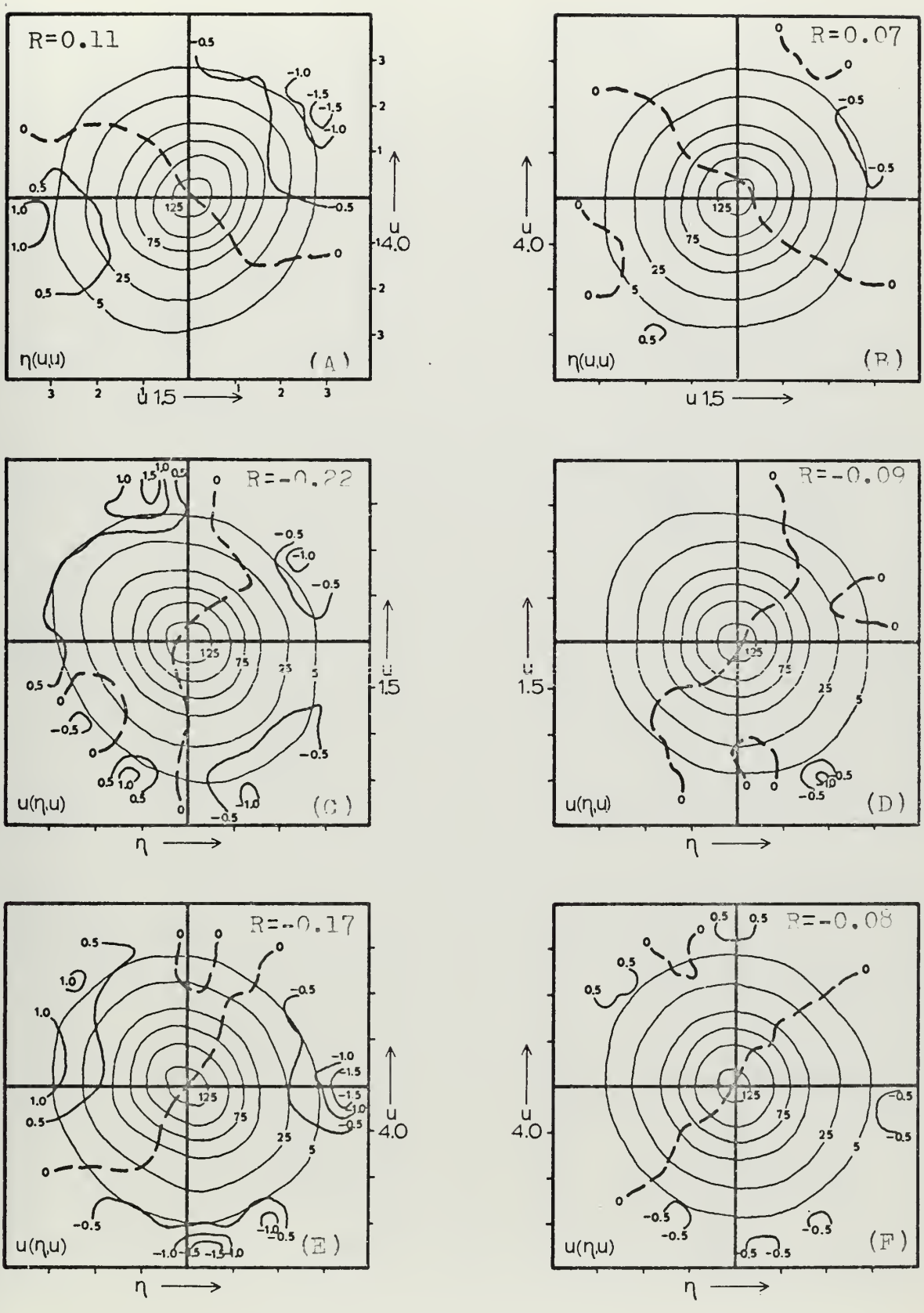

FIGURE 32. JDF/CMF Results; $U_{1.5}$ and $U_{4\ 0}$ with Waves for 19 August 1968.

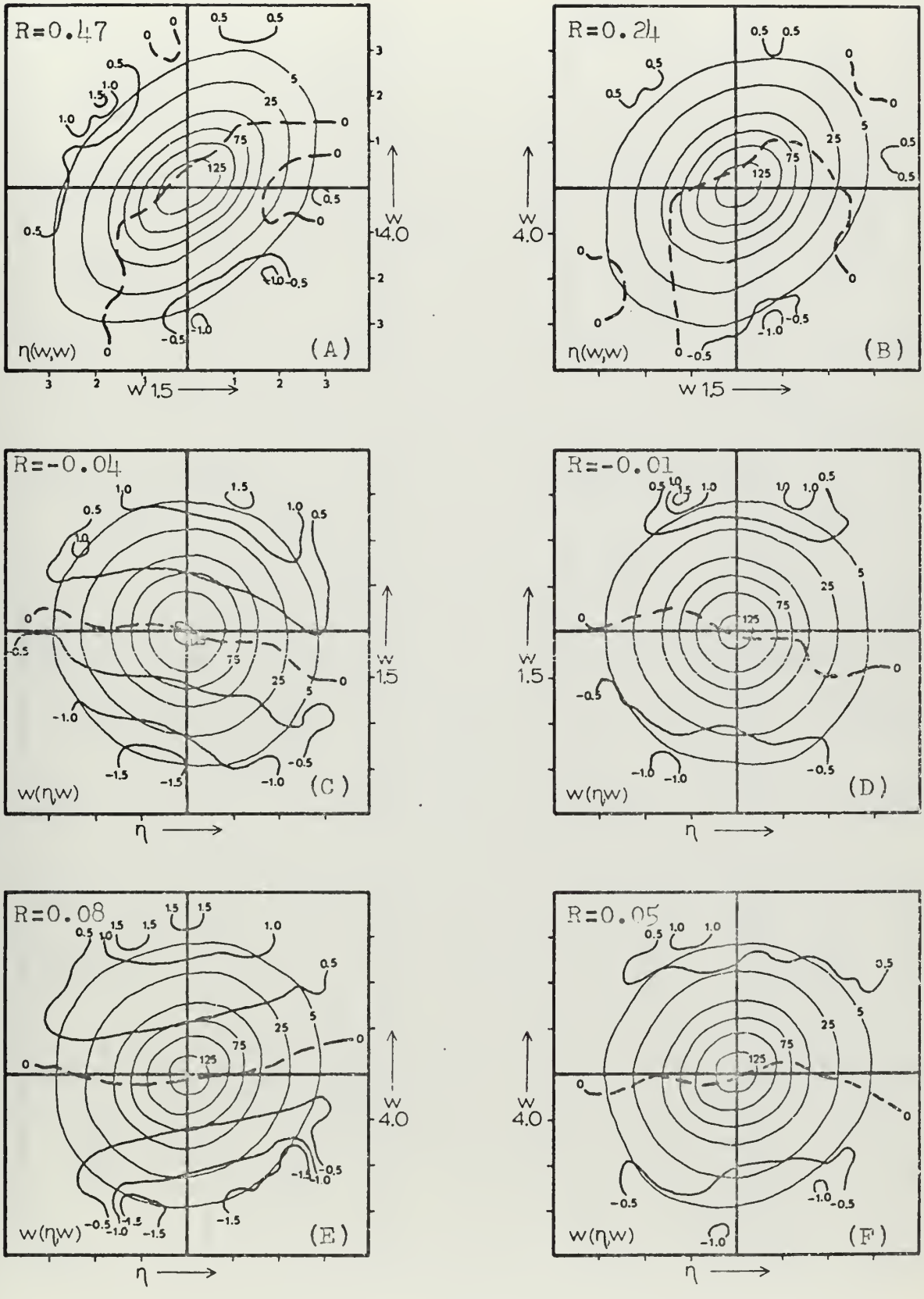

FIGURE 33. JDF/CMF Results; $W_{1.5}$ and $W_{4.0}$ with Waves for 19 August 1968.

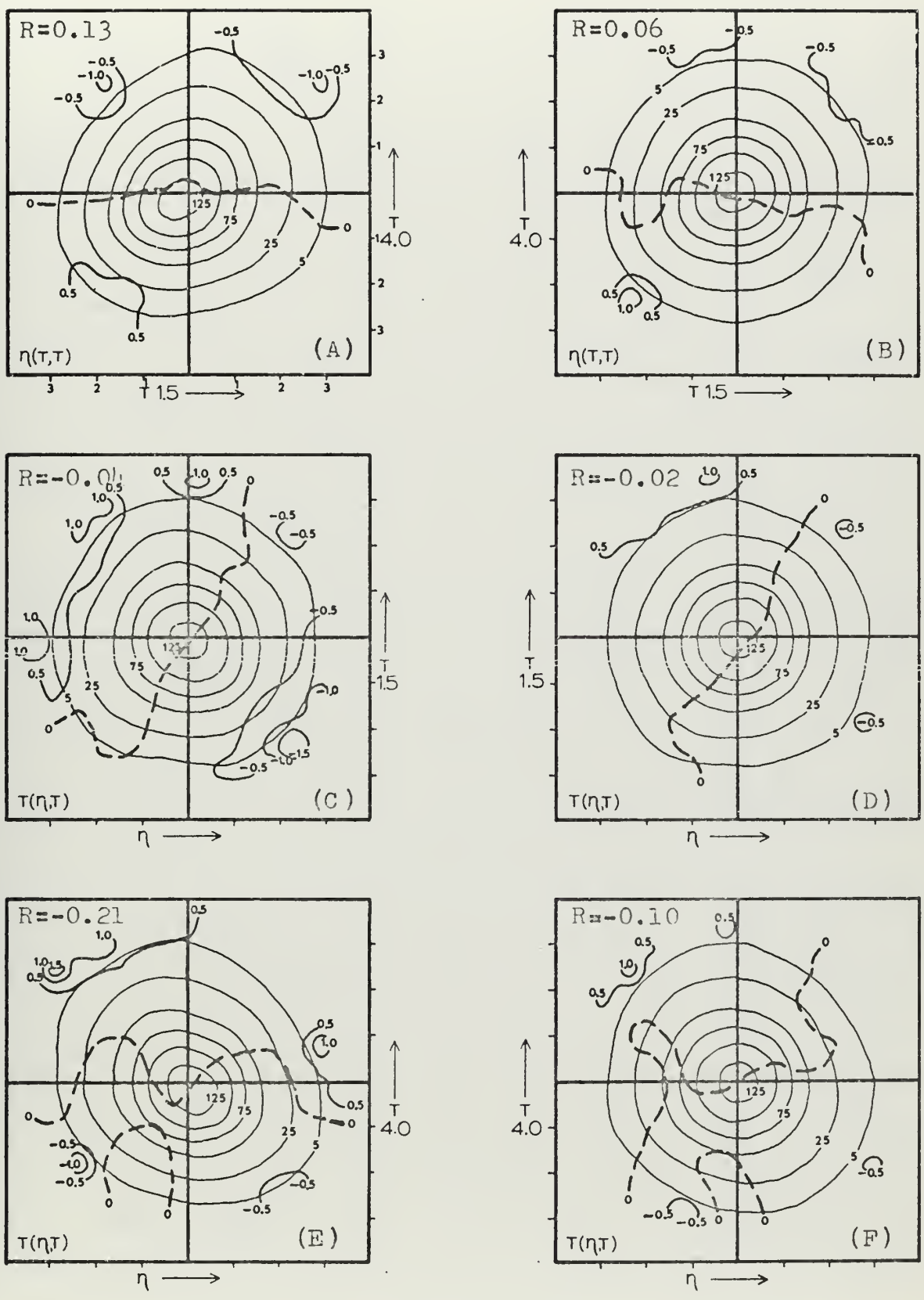

FIGURE 34. JDF/CMF Results; $T_{1.5}$ and $T_{4.0}$ with Waves for 19 August 1968.

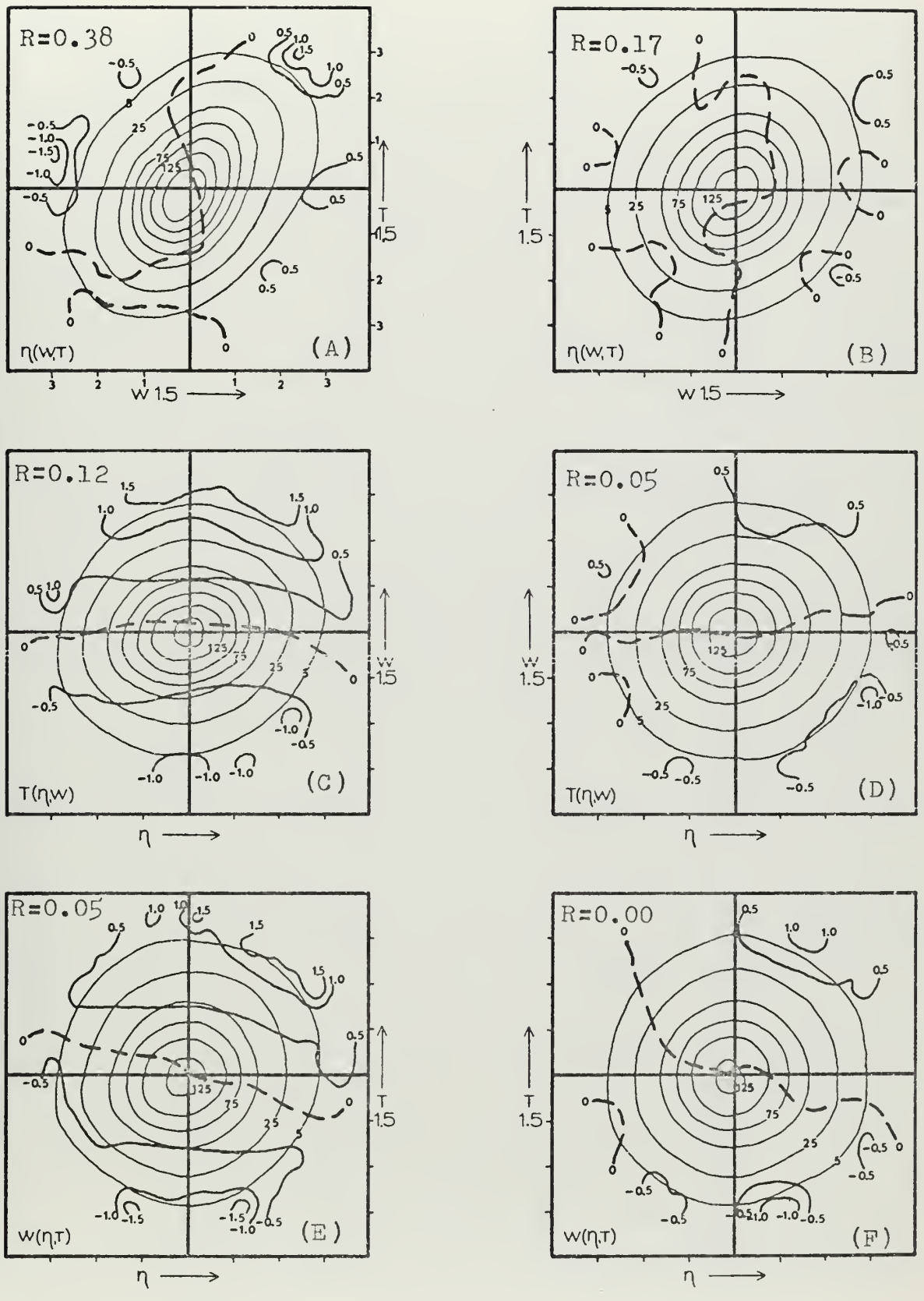

FIGURE 35. JDF/CMF Results; $W_{1.5}$ and $T_{1.5}$ with Waves for 26 September 1968.

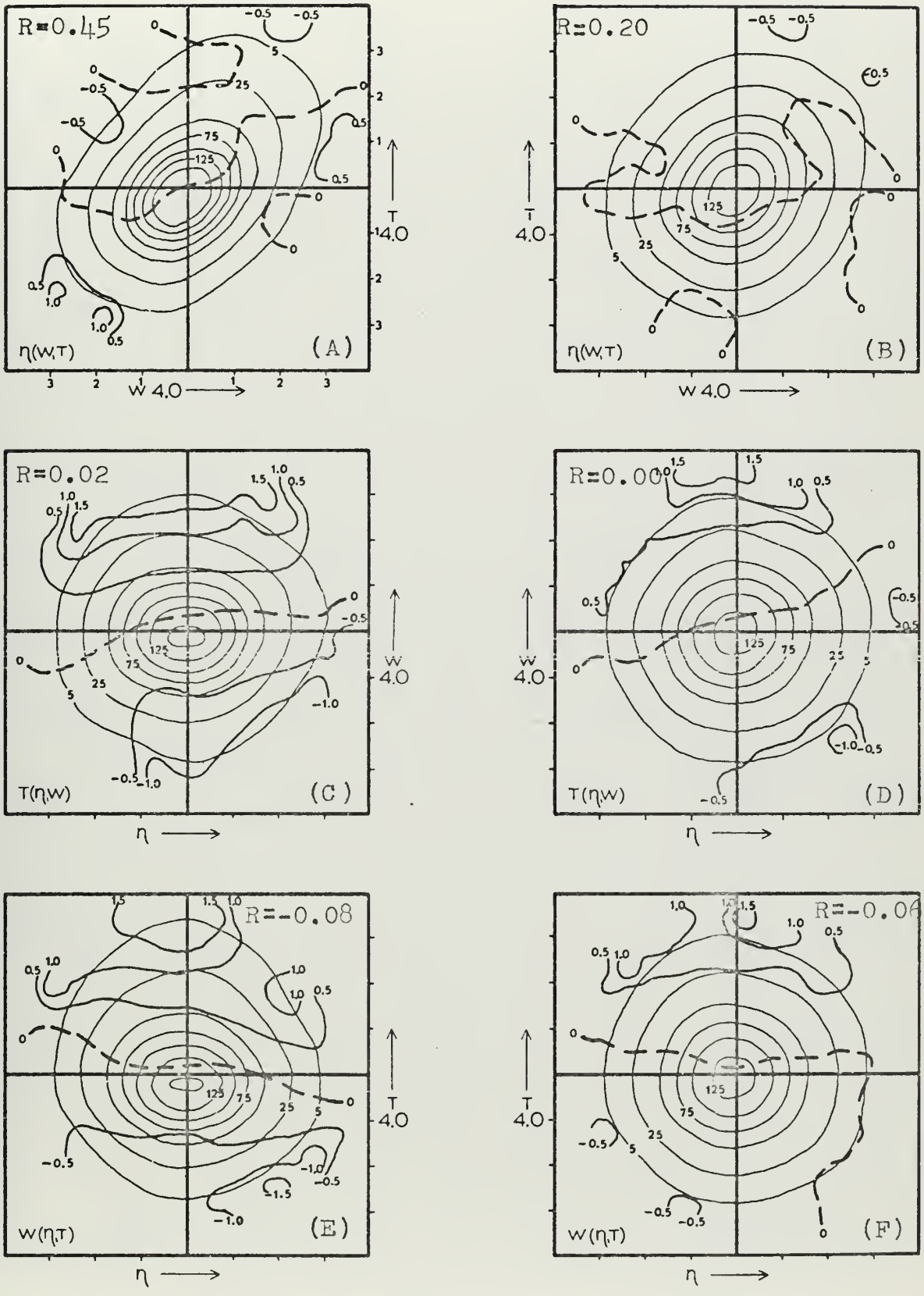

FIGURE 36. JDF/CMF Results; $W_{4.0}$ and $T_{4.0}$ with Waves for 26 September 1968.

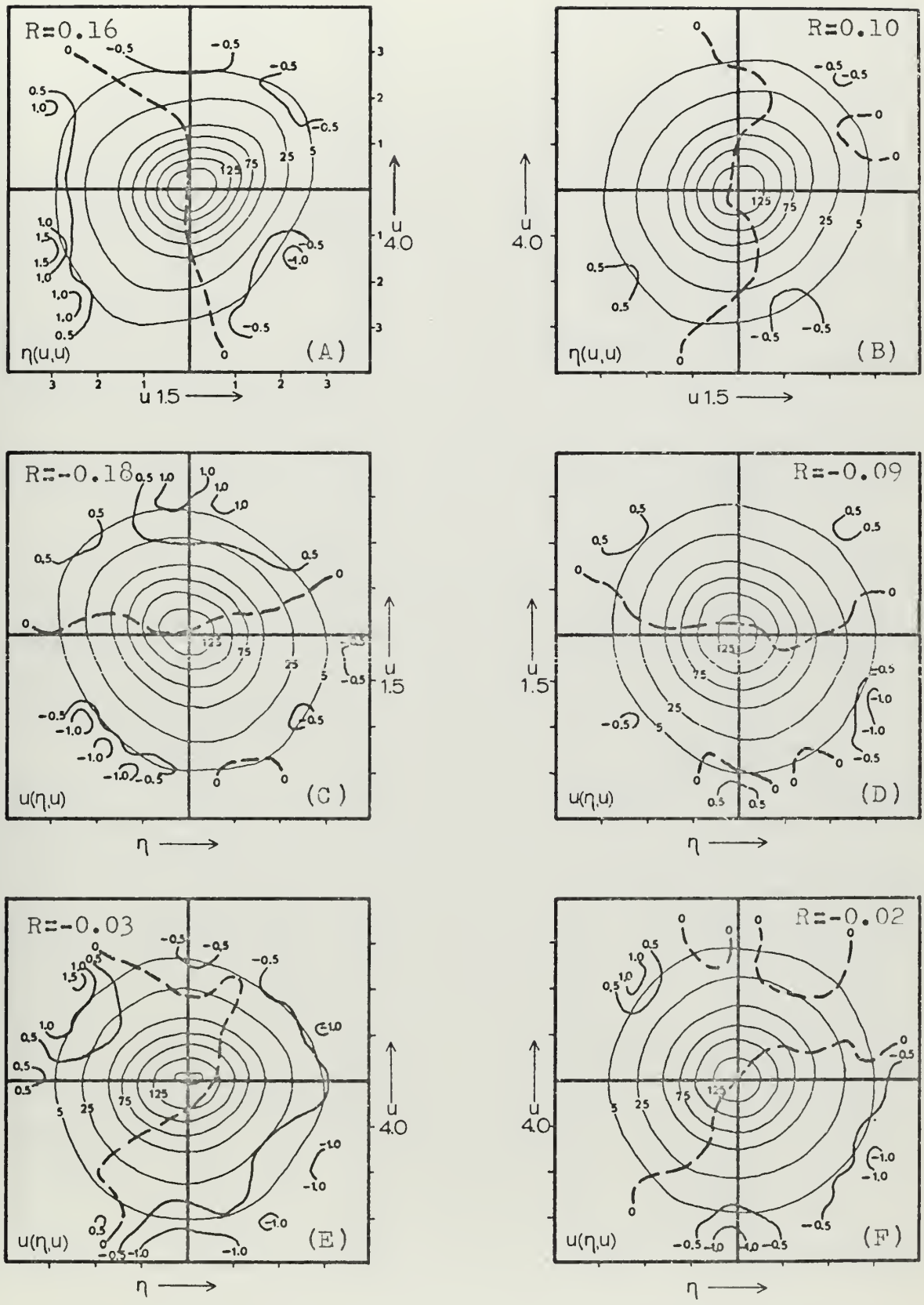

FIGURE 37. JDF/CMF Results; $U_{1.5}$ and $U_{4.0}$ with Waves for 26 September 1968.

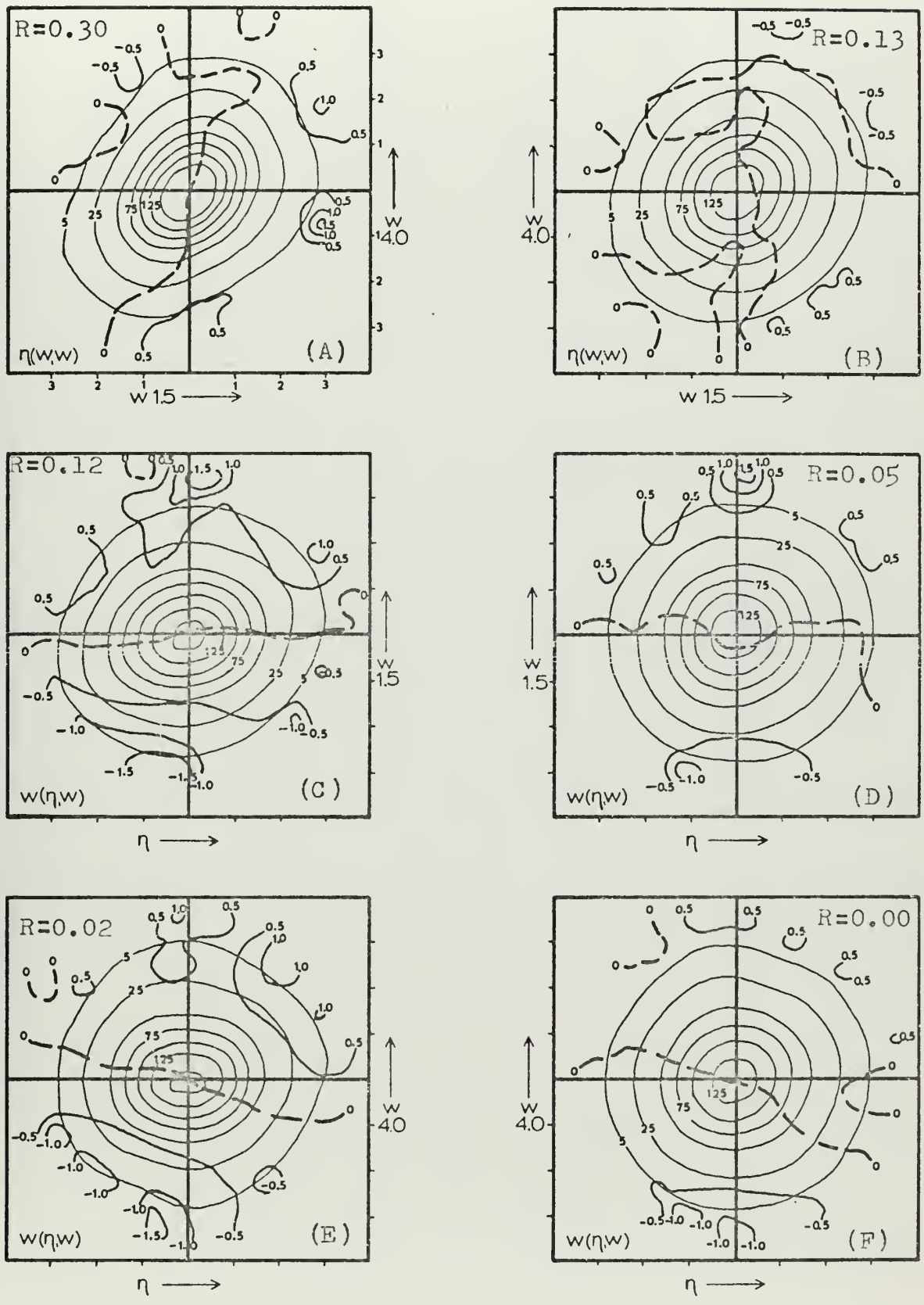

FIGURE 38. JDF/CMF Results; $W_{1.5}$ and $W_{4.0}$ with Waves for 26 September 1968.

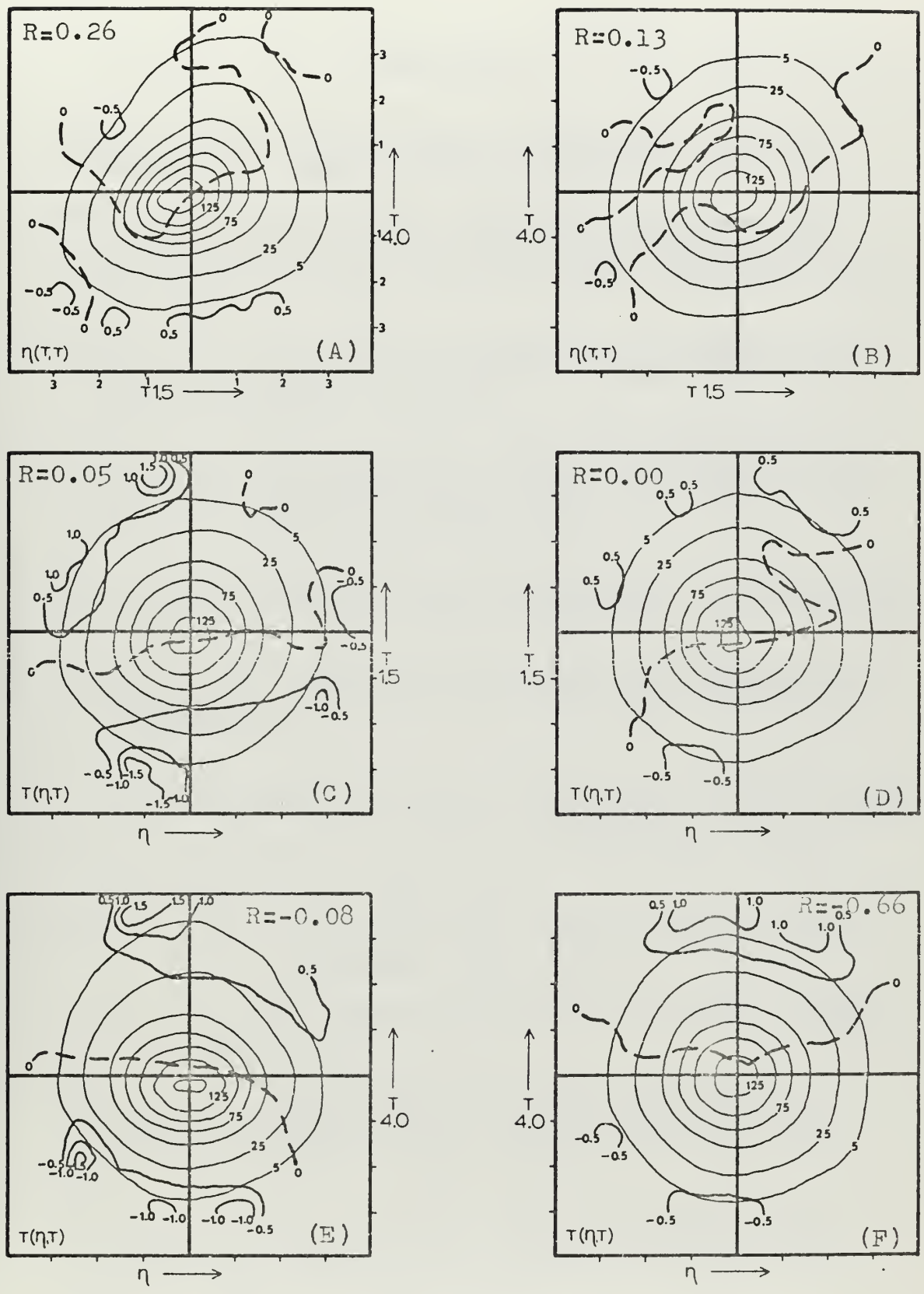

FIGURE 39. JDF/CMF Results; $T_{1.5}$ and $T_{4.0}$ with Waves for 26 September 1968.

BIBLIOGRAPHY

1. Batchelor, G. K., 1953: The Theory of Homogeneous Turbulence, Cambridge, Eng., Cambridge University Press.

2. Boston, N. E. J., et.al., 1969: Temperature Fluctuations Above an Air-Water Interface, Naval Ordnance Systems Command Project ORDTASK ORD-03C-005/561-1/UR104-03-01, Naval Postgraduate School, Unpublished.

3. Davidson, K. L., 1970: An Investigation of the Influence of Water Waves on the Adjacent Airflow. ONR Contract No. N00014-67-A-0181-0005, University of Michigan.

4. Davidson, K. L., and D. J. Portman, 1970: The Influence of Water Waves on the Adjacent Airflow, presented at Symposium on Air-Sea Interaction, XV General Assembly of IUGG, Moscow, Russia, 9-12 August, to be submitted for publication.

5. Davis, G. M., Measurement of Air Temperature and Wind Velocity from One to Eighty Centimeters Above the Sea Surface. Master's Thesis, Naval Postgraduate School, 110 pp., October 1969.

6. Kinsman, B., 1965: Wind-Waves, Their Generation and Propagation on the Ocean Surface, Englewood Cliffs, New Jersey, Prentice-Hall, Inc., 676 pp.

7. Lighthill, M. J., 1962: Physical Interpretation of the Mathematical Theory of Wave Generation by Wind, J. Fluid Mech., 14(3), 385-398.

8. Miles, J. W., 1957: On the Generation of Surface Waves by Shear Flows, J. Fluid Mech., 3(2), 185-204.

9. Miles, J. W., 1959: On the Generation of Surface Waves by Shear Flows, Part 2, J. Fluid Mech., 6(4), 568-582.

10. Stewart, R. W., 1967: Mechanics of the Air-Sea Interface. Physics of Fluids Supplement, 10, S189-S194.

11. Volkov, Y. A., 1969: The Spectra of Velocity and Temperature Fluctuations in Airflow above the Agitated Sea Surface. IZV, Atmospheric and Oceanic Physics, Academy of Sciences, USSR, 5(12), Eng. Trans. by J. Findlay, 723-731.

12. Yefimov, V. V. and V. L. Pososhkov, 1970: The Dynamics of Wave Disturbances of the Atmospheric Boundary Layer by Swell. IZV, Atmospheric and Oceanic Sciences, Academy of Sciences, USSR, 6(6), Eng. Trans. J. Findlay, 358-362.

13. Yefimov, V. V. and A. A. Sizov, 1969: Experimental Study of the Field of Wind Velocity over Waves. IZV, Atmospheric and Oceanic Sciences, Academy of Sciences, USSR, 5(9), Eng. Trans. A. Peiperl, 530-537.

INITIAL DISTRIBUTION LIST

		No. Copies
1.	Defense Documentation Center Cameron Station Alexandria, Virginia 22314	2
2.	Library, Code 0212 Naval Postgraduate School Monterey, California 93940	2
3.	Professor Kenneth Davidson, Code 51Ds Department of Meteorology Naval Postgraduate School Monterey, California 93940	5
4.	Professor Noel Boston, Code 58Bb Department of Oceanography Naval Postgraduate School Monterey, California 93940	1
5.	Lieutenant Commander Allen J. Frank, USN Box 431 Nickerson, Kansas 67561	3
6.	Professor Edward Thornton, Code 58Tm Department of Oceanography Naval Postgraduate School Monterey, California 93940	1
7.	Department of Meteorology Naval Postgraduate School Monterey, California 93940	2
8.	Professor G. J. Haltiner Department of Meteorology Naval Postgraduate School Monterey, California 93940	1
9.	Professor R. L. Alberty Department of Meteorology Naval Postgraduate School Monterey, California 93940	1
10.	Professor R. L. Elsberry Department of Meteorology Naval Postgraduate School Monterey, California 93940	1

11. Dr. Donald J. Portman 1
Department of Meteorology and Oceanography
University of Michigan
Ann Arbor, Michigan 48103

12. Professor R. T. Williams 1
Department of Meteorology
Naval Postgraduate School
Monterey, California 93940

Security Classification

DOCUMENT CONTROL DATA - R & D

(Security classification of title, body of abstract and indexing annotation must be entered when the overall report is classified)

1. ORIGINATING ACTIVITY (Corporate author)
Naval Postgraduate School
Monterey, California 93940

2a. REPORT SECURITY CLASSIFICATION
Unclassified

2b. GROUP

3. REPORT TITLE
An Investigation of the Properties and Influence of Wave-Induced Organized Motion in the Adjacent Airflow

4. DESCRIPTIVE NOTES (Type of report and, inclusive dates)
Master's Thesis; September 1971

5. AUTHOR(S) (First name, middle initial, last name)
Allen Jesten Frank

6. REPORT DATE	7a. TOTAL NO. OF PAGES	7b. NO. OF REFS
September 1971	84	13

8a. CONTRACT OR GRANT NO.	9a. ORIGINATOR'S REPORT NUMBER(S)
b. PROJECT NO.	
c.	9b. OTHER REPORT NO(S) (Any other numbers that may be assigned this report)
d.	

10. DISTRIBUTION STATEMENT
Approved for public release; distribution unlimited.

11. SUPPLEMENTARY NOTES	12. SPONSORING MILITARY ACTIVITY
	Naval Postgraduate School Monterey, California 93940

13. ABSTRACT

Turbulence data obtained over natural water waves were analyzed using joint probability distribution and conditional means methods. These data represented conditions when the waves were decaying and when the waves were building. In both cases, significant wave-induced fluctuations were identified in the airflow. All features of the velocity fluctuations were examined for two levels above mean water level. In the case of a decaying wave field, decelerations in the airflow can be associated with an assumed propagating pressure maximum over the crest of the wave. Other than this deceleration, the airflow appears to reflect simple streamline bending over the mobile irregular wave surface. In the case of a building wave field, velocity fluctuations appear to agree with those predicted by linear wave generating theories.

DD FORM 1 NOV 65 1473 (PAGE 1)
S/N 0101-807-6811

Security Classification

1-31408

KEY WORDS	LINK A		LINK B		LINK C	
	ROLE	WT	ROLE	WT	ROLE	WT
Turbulence						
Wave-induced motion						
Joint probability density function						
Conditional mean function						
Phase-amplitude						

BINDERY

Thesis
F782
c.1

130757

Frank

An investigation of the properties and influence of wave-induced organized motion in the adjacent airflow.

BINDERY

Th
F7
c.

Thesis
F782
c.1

130757

Frank

An investigation of the properties and influence of wave-induced organized motion in the adjacent airflow.

thesF782
An investigation of the properties and i
3 2768 001 95981 0
DUDLEY KNOX LIBRARY